



Research article

Integrative genomic analysis of a novel small nucleolar RNAs prognostic signature in patients with acute myelocytic leukemia

Rui Huang¹, Xiwen Liao² and Qiaochuan Li^{1,*}

¹ Department of Hematology, The First Affiliated Hospital of Guangxi Medical University, Nanning 530021, China

² Department of Hepatobiliary Surgery, The First Affiliated Hospital of Guangxi Medical University, Nanning 530021, China

* **Correspondence:** Email: liqiaochuan@sohu.com; Tel: +867715356746; Fax: +867715352681.

Abstract: This study mainly used The Cancer Genome Atlas (TCGA) RNA sequencing dataset to screen prognostic snoRNAs of acute myeloid leukemia (AML), and used for the construction of prognostic snoRNAs signature for AML. A total of 130 AML patients with RNA sequencing dataset were used for prognostic snoRNAs screening. SnoRNAs co-expressed genes and differentially expressed genes (DEGs) were used for functional annotation, as well as gene set enrichment analysis (GSEA). Connectivity Map (CMap) also used for potential targeted drugs screening. Through genome-wide screening, we identified 30 snoRNAs that were significantly associated with the prognosis of AML. Then we used the step function to screen a prognostic signature composed of 14 snoRNAs (SNORD72, SNORD38, U3, SNORA73B, SNORD79, SNORA73, SNORD12B, SNORA74, SNORD116-12, SNORA65, SNORA14, snoU13, SNORA75, SNORA31), which can significantly divide AML patients into high- and low-risk groups. Through GSEA, snoRNAs co-expressed genes and DEGs functional enrichment analysis, we screened a large number of potential functional mechanisms of this prognostic signature in AML, such as phosphatidylinositol 3-kinase-Akt, Wnt, epithelial to mesenchymal transition, T cell receptors, NF-kappa B, mTOR and other classic cancer-related signaling pathways. In the subsequent targeted drug screening using CMap, we also identified six drugs that can be used for AML targeted therapy, they were alimemazine, MG-262, fluoxetine, quipazine, naltrexone and oxybenzone. In conclusion, our current study was constructed an AML prognostic signature based on the 14 prognostic snoRNAs, which may serve as a novel prognostic biomarker for AML.

Keywords: small nucleolar RNA; RNA sequencing; acute myeloid leukemia; the cancer genome atlas; prognostic signature

1. Introduction

As a clonal malignant disease of hematopoietic system, acute myeloid leukemia (AML) is a group of diseases with high heterogeneity [1,2]. In recent years, with the development of immunology, cytogenetics and molecular biology, the biological characteristics of AML tumor cells have been more deeply understood and laid a foundation for the precise classification, diagnosis, prognosis and selection of the best treatment for AML [3–6]. Epidemiological studies have shown that environmental, occupational and genetic factors are closely related to the incidence of AML [7,8]. Small nucleolar RNA (snoRNA) is also a class of non-coding RNA, with a length of 60-30nt. As early studies found that snoRNA was mainly located in the nucleoli and was related to the processing and modification of rRNA, its function was relatively simple [9–11]. However, in recent years, more and more RNA sequencing (RNA-seq) dataset show that snoRNA shows a general trend of high expression in tumors, and some studies show that snoRNA is involved in the occurrence, progression and prognosis of tumors, and may be a kinds of new clinical biomarkers [12–14]. Gong et al. organized The Cancer Genome Atlas (TCGA) pan-cancer RNA-seq datasets and turned the analyzed snoRNA datasets into a visual webpage for researchers to analyze the relationship between snoRNAs and cancers [15]. Through literature search, we have not found any related research on the relationship between snoRNAs and AML prognosis. To fill in this research gap, we extracted the snoRNA dataset from the RNA-seq dataset of TCGA AML cohort, and used to screen for the prognostic snoRNAs of AML, and explored their related molecular mechanisms. This study mainly used TCGA RNA sequencing dataset to screen prognostic snoRNAs of AML, and used for the construction of prognostic signature for AML.

2. Materials and methods

2.1. Data acquisition and processing

Level 3 RNA-seq dataset was downloaded from TCGA website (<https://portal.gdc.cancer.gov>), and the corresponding clinical parameters were obtained from University of California, Santa Cruz (UCSC) Xena (<http://xena.ucsc.edu>) [16]. Inclusion criteria for this study were that AML patients with complete prognostic parameters and RNA sequencing data sets would be included in the follow-up prognostic analysis of this study, otherwise they will be excluded. The raw RNA-seq dataset was normalized with *edgeR* [17]. SnoRNA is included in the RNA-seq dataset. We download genome annotation files from the Ensembl website (<http://asia.ensembl.org/index.html>) to annotate the genes and snoRNAs in the RNA-seq matrix. Then separate the snoRNAs from the RNA-seq matrix according to the annotated file. Prognostic snoRNAs were identified by the multivariate Cox proportional hazards regression model using the *survival* package in the R platform. Then we used *step* function and Cox model to screen the optimal prognostic signature in R platform. The calculation formula of prognostic signature is as follows: risk score = $\text{ExpsnoRNA}_1 \times \beta_{\text{snoRNA}_1} + \text{ExpsnoRNA}_2 \times \beta_{\text{snoRNA}_2} + \dots + \text{ExpsnoRNA}_n \times \beta_{\text{snoRNA}_n}$ (Exp: expression value) [18–20]. The

time-dependent receiver operating characteristic curve is realized by the *survivalROC* package in the R platform. The nomogram was implemented by the *rms* package of R platform. Since all datasets of gastric cancer included in the present study were downloaded from open access public database, and the authors were not involved in any animal or human experiments. Therefore, additional approval by an Ethics Committee was not needed.

2.2. Functional enrichment analysis

The co-expression genes screening of snoRNAs are realized by *Cor* function of R platform. Pearson correlation coefficient $|r| > 0.4$ and P value < 0.05 was identified as the co-expressed genes of snoRNA. Functional enrichment analysis was performed using Database for Annotation, Visualization, and Integrated Discovery v6.8 (DAVID v6.8, <https://david.ncifcrf.gov/home.jsp>) [21]. We also used the gene set enrichment analysis (GSEA) approach to perform differential functional enrichment analysis for AML patients between high-risk and low-risk phenotypes. Gene set database of GSEA were used the c2 (curated gene sets: c2.all.v7.0.symbols.gmt) and c5 (gene ontology gene sets: c5.all.v7.0.symbols.gmt) gene set, which were downloaded from the molecular signatures database [22–25]. GSEA results of $|\text{normalized enrichment score (NES)}| > 1$, P value < 0.05 and false discovery rate (FDR) < 0.25 were considered to be statistically significant. We then used *edgeR* packages to screen differentially expressed genes (DEGs) between AML patients with high- and low-risk phenotypes. Genes with $|\log_2 \text{fold change (FC)}| > 2$, P value < 0.05 and FDR < 0.05 were identified as DEGs. After screening DEGs, we also use these DEGs and Connectivity Map (CMap: <https://portals.broadinstitute.org/cmap/>) online analysis tools to screen potential AML targeted therapeutic drugs [26,27]. The chemical formula of the drug is obtained from the PubChem website (<https://pubchem.ncbi.nlm.nih.gov>) [28,29], and the gene-drug interaction network were obtained from the STITCH website (<http://stitch.embl.de/>) [30–32]. We further used the Estimation of STromal and Immune cells in MAlignant Tumor tissues using Expression data (ESTIMATE) method to score the immune cells and stromal cells in the tumor microenvironment [33]. CIBERSORT was used for immune cell infiltration analysis [34].

2.3. Statistical analysis

The grouping of high- and low-expression groups are based on the median expression value of each gene. In this study, FDR was calculated in strict accordance with the Benjamini-Hochberg program [35]. Volcano plot and heat map are drawn in R platform by *ggplot2* package in the R platform (Version 3.6.2, <https://www.r-project.org>) and interactive network diagrams are drawn using Cytoscape software (Version 3.6.1, <https://cytoscape.org>) [36,37]. $P < 0.05$ was considered to be statistically significant.

3. Results

3.1. Pronostic snoRNAs screening

The flow chart of this study is shown in Figure 1. There were 130 AML patients of TCGA cohort were included into our current study, the clinical parameters were shown in Table 1. In the obtained clinical parameters, we found that age and french american british (FAB) morphology type

were significantly related to the prognosis of AML. Subsequently, we also conducted survival analysis based on ALP classification and found that APL patients had a better prognosis than non-APL patients ($P = 0.003$, Table 1). We included these two parameters in the subsequent multivariate Cox proportional hazard regression model for adjustment. A total of 940 snoRNAs were derived from the RNA-seq dataset. After normalization by edgeR, we finally obtained 354 snoRNAs with an average value greater than 1 for subsequent survival analysis. By using the survival package of the R platform, we screened a total of 30 snoRNAs in the TCGA cohort that were significantly related to the prognosis of AML (Figure 2 and Table S1).

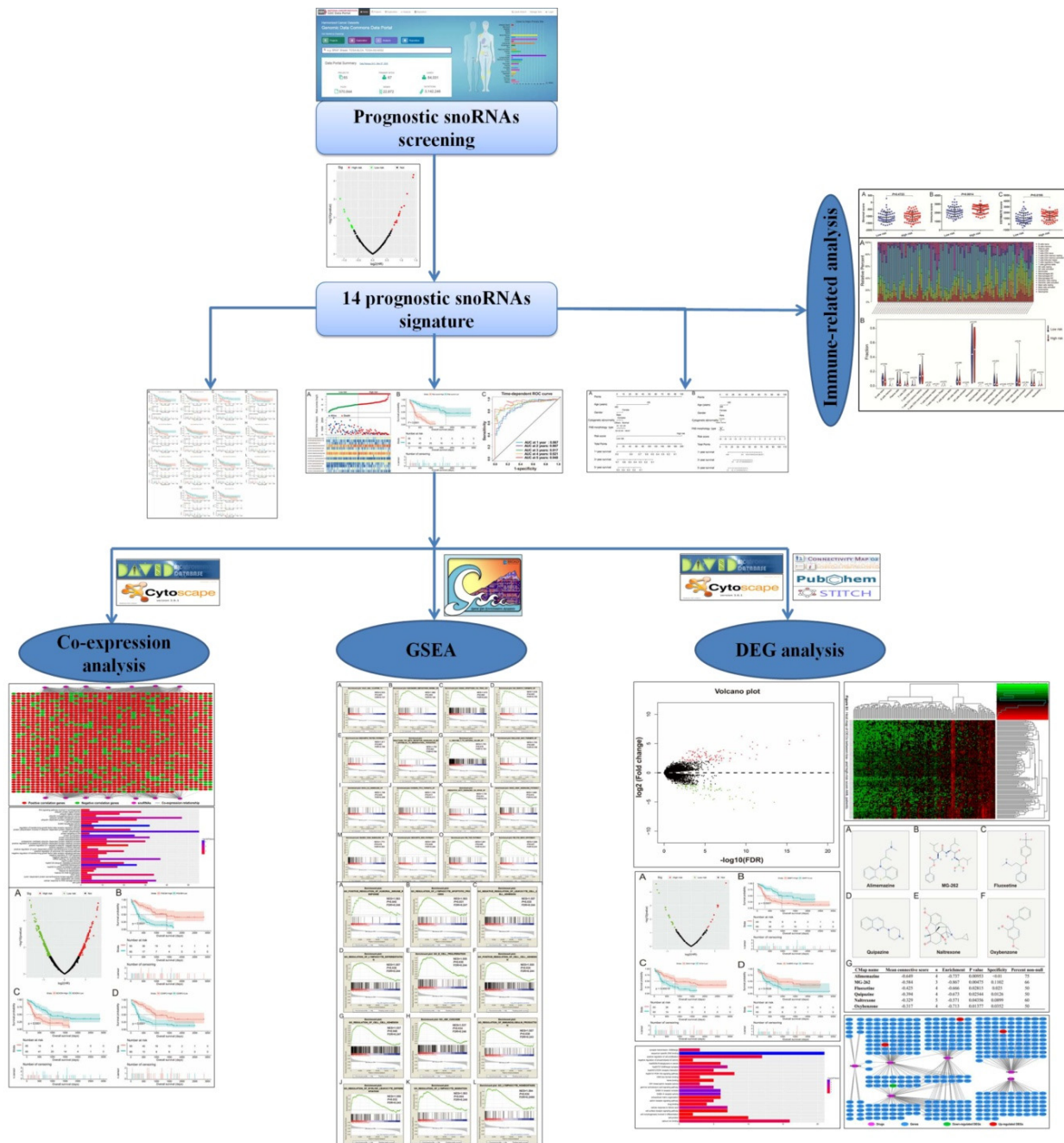


Figure 1. Flow chart of the present study.

Table 1. Clinical parameters of 130 AML patients in TCGA cohort.

Variables	Events/total (n = 130)	MST (days)	HR (95% CI)	Log-rank <i>P</i>
Age (years)				< 0.0001
≤ 65	48/96	822	1	
> 65	30/34	214	3.236(2.022–5.180)	
Gender				0.916
Female	36/60	671	1	
Male	42/70	577	0.976(0.625–1.526)	
Cytogenetics abnormality §				0.19
Normal	42/61	518	1	
Complex	8/15	366	0.984(0.460–2.105)	
Others	21/42	945	0.625(0.369–1.056)	
FAB morphology type				0.029
M0	7/12	792	1	
M1	19/30	731	1.438(0.604–3.424)	
M2	19/32	486	1.240(0.520–2.955)	
M3	3/14	NA	0.278(0.072–1.083)	
M4	19/27	580	1.451(0.609–3.458)	
M5	8/12	214	2.027(0.728–5.644)	
M6 + M7	3/3	304	3.361(0.851–13.272)	
FAB morphology type (APL classification)				0.003
APL	3/14	NA	1	
Non-APL	75/116	518	4.965(1.554–15.867)	
Risk score				< 0.0001
Low risk	24/65	1706	1	
High risk	54/65	245	6.761(3.911–11.687)	

Notes: §Information of cytogenetics abnormality was unavailable in 12 patients.

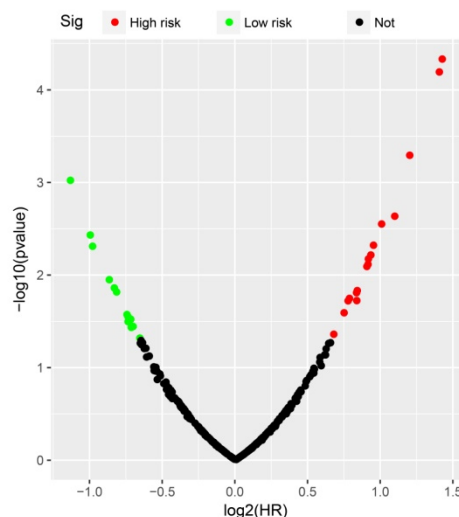


Figure 2. Volcano plot of prognostic snoRNAs screening.

3.2. Prognostic signature and nomogram construction

Then we used the step function in the R platform to screen the optimal prognostic signature model, and finally screened out 14 prognostic snoRNAs combinations in the TCGA AML cohort, which can significantly divide AML patients into high-risk and low-risk patients (Figure 3A–C, Table 1, log-rank $P < 0.0001$, median survival time of low risk vs. high risk = 1706 vs. 245 days). These 14 prognostic snoRNAs were SNORD72, SNORD38, U3, SNORA73B, SNORD79, SNORA73, SNORD12B, SNORA74, SNORD116-12, SNORA65, SNORA14, snoU13, SNORA75, SNORA31. The risk score model formula is as follows: risk score = $\text{Exp}_{\text{SNORD72}} \times 0.452 + \text{Exp}_{\text{SNORD38}} \times 0.310 + \text{Exp}_{\text{U3}} \times (-0.203) + \text{Exp}_{\text{SNORA73B}} \times 0.527 + \text{Exp}_{\text{SNORD79}} \times (-0.288) + \text{Exp}_{\text{SNORA73}} \times (-0.712) + \text{Exp}_{\text{SNORD12B}} \times (-0.608) + \text{Exp}_{\text{SNORA74}} \times 0.226 + \text{Exp}_{\text{SNORD116-12}} \times (-0.540) + \text{Exp}_{\text{SNORA65}} \times 1.227 + \text{Exp}_{\text{SNORA14}} \times 0.290 + \text{Exp}_{\text{snoU13}} \times 0.756 + \text{Exp}_{\text{SNORA75}} \times 0.225 + \text{Exp}_{\text{SNORA31}} \times (-0.282)$. After correcting age and FAB morphology type in the multivariate Cox proportional hazards regression model, we found that AML patients with high risk score had a significantly increased risk of death than these with lower risks (adjusted $P < 0.0001$, adjusted hazard ratio = 5.967, 95% confidence interval = 3.319-10.728). The time-dependent ROC curve indicated that this prognostic signature had a high accuracy in predicting survival for AML patients [all area under the curve (AUC) were greater than 0.8], especially the highest accuracy in predicting 5-year survival for AML patients, which the AUC was 0.940 (Figure 3C). The Kaplan-Meier survival curves of the 14 snoRNAs that make up the prognostic signature were summarized in Figure 4A–N. Then we constructed the AML prognosis nomogram according to the risk value and phenotype of risk score, we found that the risk score contributed the most to AML prognosis than other clinical parameters (Figure 5A,B).

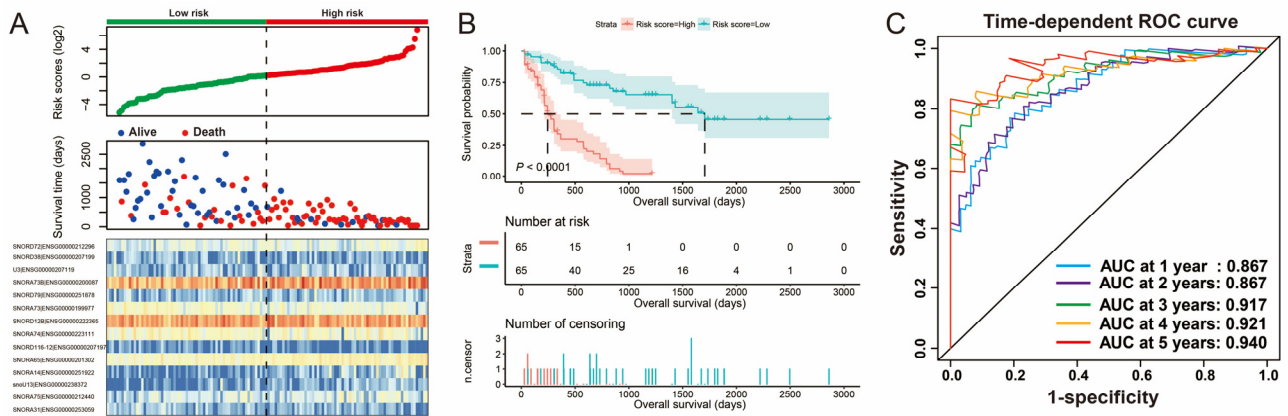


Figure 3. Prognostic signature of fourteen prognostic snoRNAs in AML overall survival. (A) Survival distribution plot of fourteen prognostic snoRNAs and AML; (B) Kaplan-Meier curve of the prognostic signature; (C) Time-dependent ROC curve of the prognostic signature.

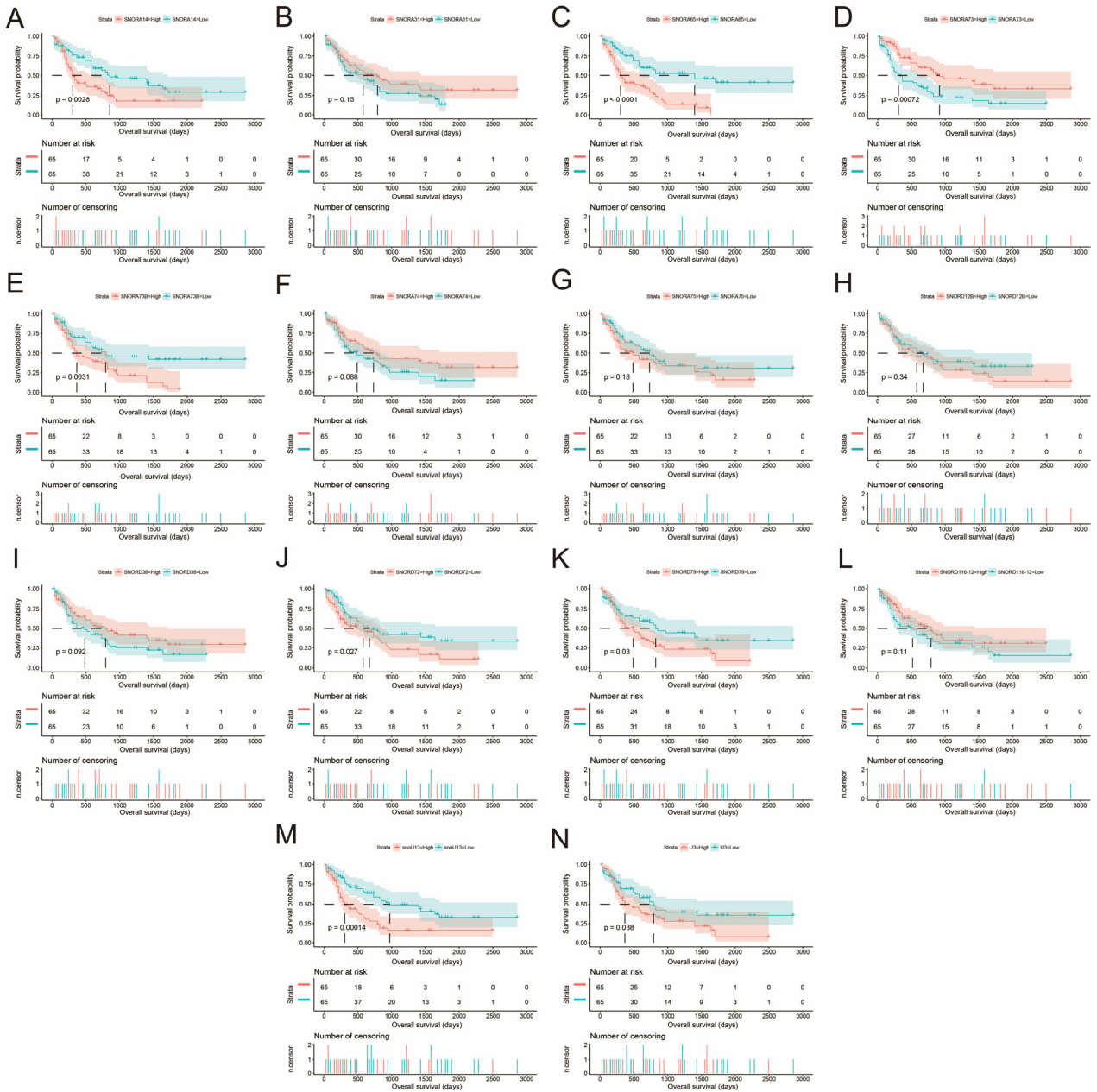


Figure 4. Kaplan-Meier curve of fourteen prognostic snoRNAs in AML. (A)SNORA14; (B) SNORA31; (C) SNORA65; (D) SNORA73; (E) SNORA73B; (F) SNORA74; (G) SNORA75; (H) SNORA12B; (I) SNORD38; (J) SNORD72; (K) SNORD79; (L) SNORD116-12; (M) snoU13; (N) U3.

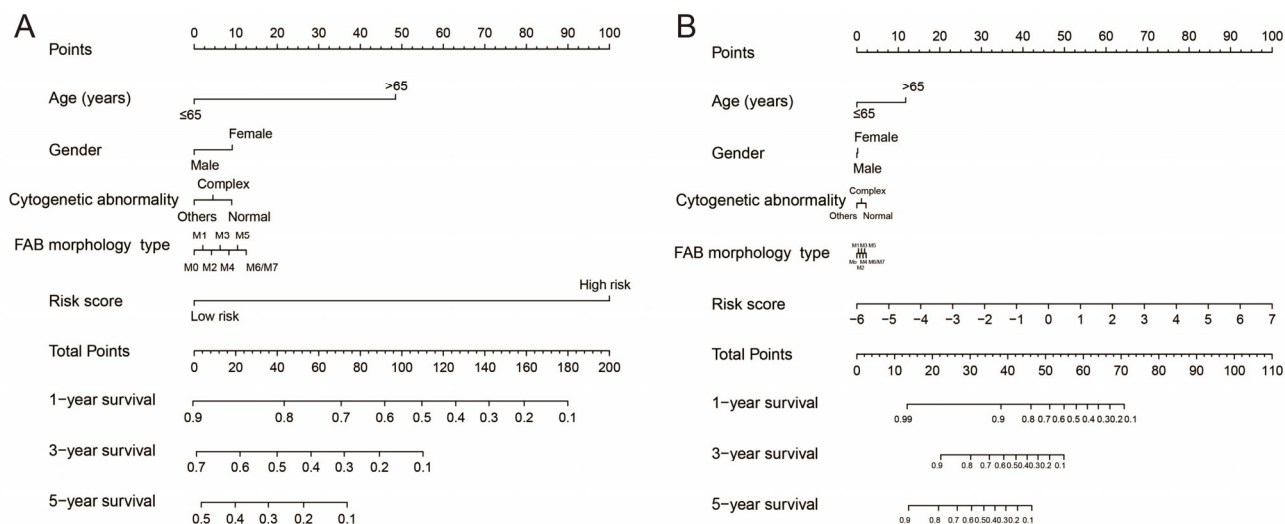


Figure 5. Nomogram of the risk score in AML overall survival. (A) Nomogram of low- and high-risk score phenotypes in AML; (B) Nomogram of the risk score in AML.

3.3. Functional enrichment analysis

In order to further understand the role of this prognostic signature in AML, we used RNA-seq dataset to screen the co-expression protein coding genes (PCGs) for snoRNAs, and then used for functional enrichment. Through co-expression analysis, we obtained a total of 1971 snoRNA-PCG co-expression interaction pairs (Figure 6, Table S2). Through DAVID v6.8 functional enrichment, we found that these snoRNAs co-expressed PCGs can be significantly enriched in protein SUMOylation, protein ubiquitination, cellular response to DNA damage stimulus, DNA repair, positive regulation of canonical Wnt signaling pathway, negative regulation of target of rapamycin (TOR) signaling, cell cycle, regulation of transforming growth factor beta receptor signaling pathway, cyclin-dependent protein serine/threonine kinase regulator activity, positive regulation of I-kappaB kinase/NF-kappaB signaling and negative regulation of autophagy (Figure 7, Table S3). We then used the survival package of the R platform to perform a prognosis analysis of these snoRNAs co-expressed PCGs using a multivariate Cox proportional hazard regression model. In total, we obtained 382 snoRNAs co-expressed PCGs that were significantly related to the prognosis of AML (Figure 8A, Table S4). The top three genes with the most significant P values are phosphodiesterase 3B (PDE3B), branched chain keto acid dehydrogenase kinase (BCKDK) and centromere protein C (CENPC). Kaplan-meier survival curves of these three genes were shown in Figure 8B–D.

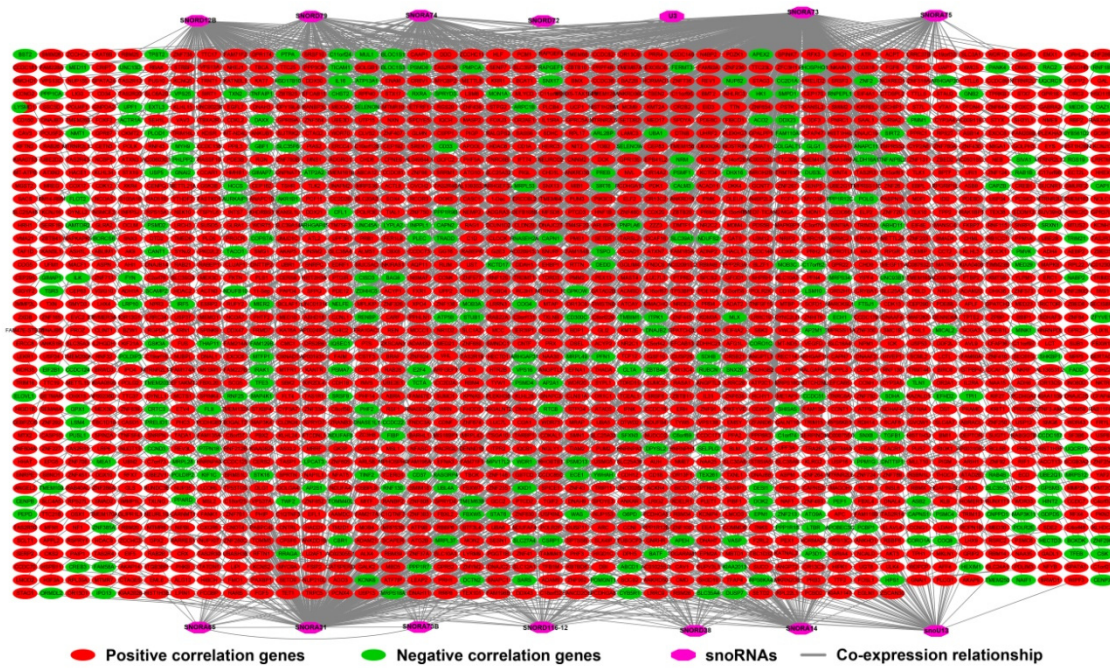


Figure 6. SnoRNA-gene co-expressed interaction networks of fourteen prognostic snoRNAs in AML.

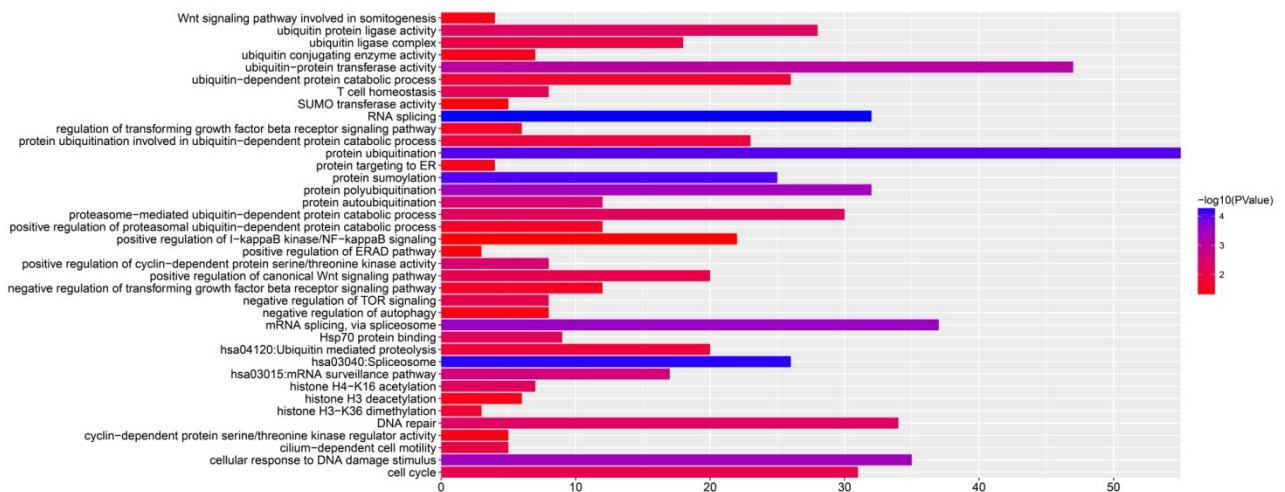


Figure 7. Functional enrichment results of the fourteen prognostic snoRNAs co-expressed genes.

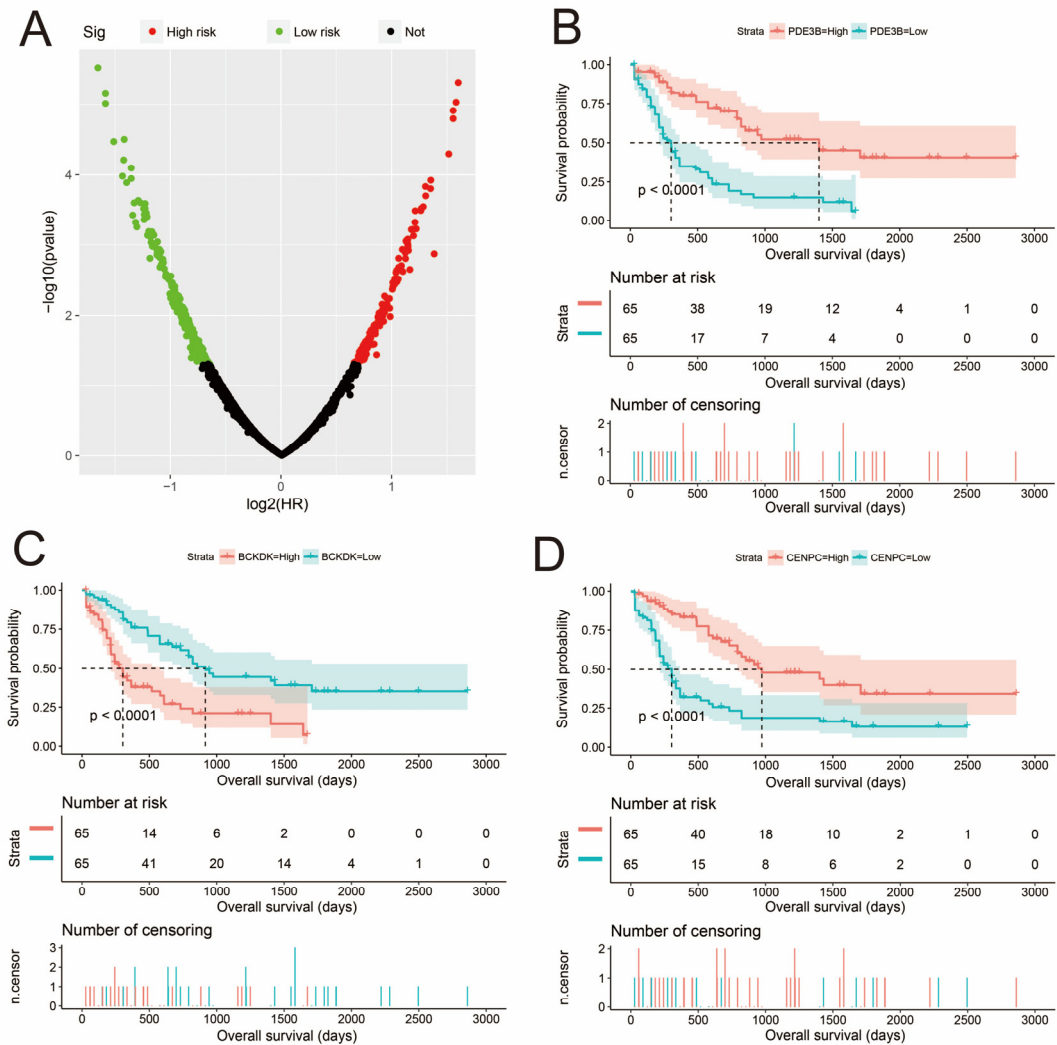


Figure 8. Survival analysis results of the fourteen prognostic snoRNAs co-expressed genes in AML. (A) Volcano plot of the survival results; (B) Kaplan-Meier curve of PDE3B; (C) Kaplan-Meier curve of BCKDK; (D) Kaplan-Meier curve of CENPC.

Then we also used GSEA to enrich the differential biological functions and pathways between high- and low-risk score phenotypes. We used c2 reference data set for pathway enrichment analysis in GSEA, and we found that high-risk phenotypes could be significantly enriched in AML cluster 15, metastasis model up, apoptosis via trail dn, mitogen-activated protein kinase 14 (MAPK14) targets up, Th1/Th2 pathway, transforming growth factor (TGF) beta receptor signaling in epithelial to mesenchymal transition (EMT), T to natural killer up, janus kinase 2 (JAK2) targets up, IL6 signaling up, tumor protein 53 (TP53) targets up, Akt1 signaling via mTOR up, vascular endothelial growth factor A (VEGF) signaling pathway, CD40 signaling up, Rho pathway, T cell receptors (TCR) pathway, and P38/Mikk3/6 pathway (Figure 9A–P, Table S5). While GSEA using c5 reference data set were significantly enriched in positive regulation of humoral immune response, regulation of lymphocyte apoptotic process, negative regulation of leukocyte cell-cell adhesion, regulation of lymphocyte differentiation, B cell proliferation, positive regulation of cell-cell adhesion, regulation of cell-cell adhesion, JUN N-terminal kinase (JNK) cascade, regulation of immunoglobulin

production, regulation of myeloid leukocyte differentiation, regulation of lymphocyte migration, and lymphocyte homeostasis (Figure 10A–L, Table S6).

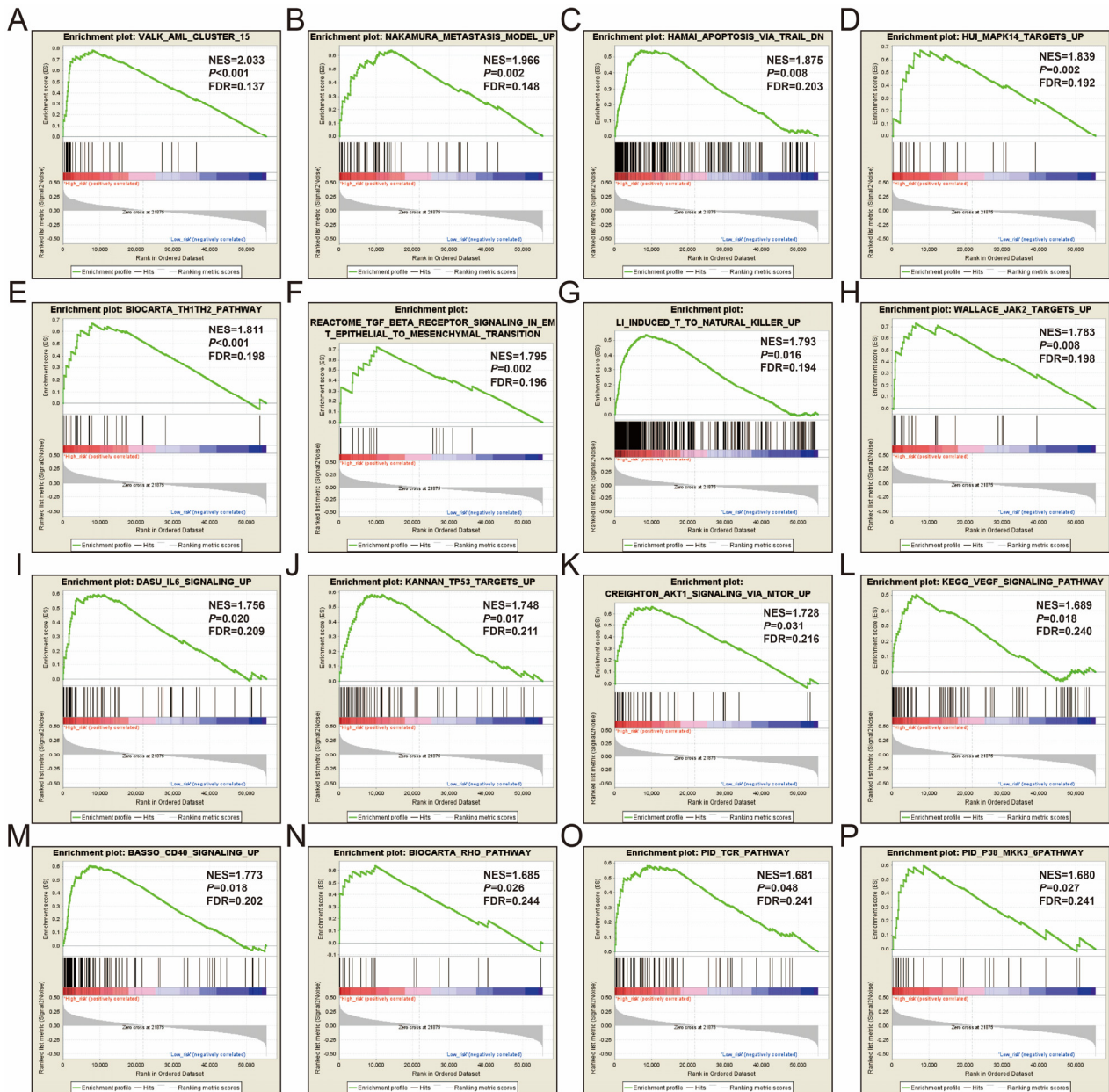


Figure 9. GSEA analysis results of the low- and high-risk score phenotypes in AML using c2 reference gene set. (A) AML cluster 15; (B) metastasis model up; (C) apoptosis via trail dn; (D) MAPK14 targets up; (E) Th1/Th2 pathway; (F) TGF beta receptor signaling in epithelial to mesenchymal transition (EMT); (G) T to natural killer up; (H) JAK2 targets up; (I) IL6 signaling up; (J) TP53 targets up; (K) Akt1 signaling via mTOR up; (L) VEGF signaling pathway; (M) CD40 signaling up; (N) Rho pathway; (O) TCR pathway; (P) P38/MIKK3/6 pathway.

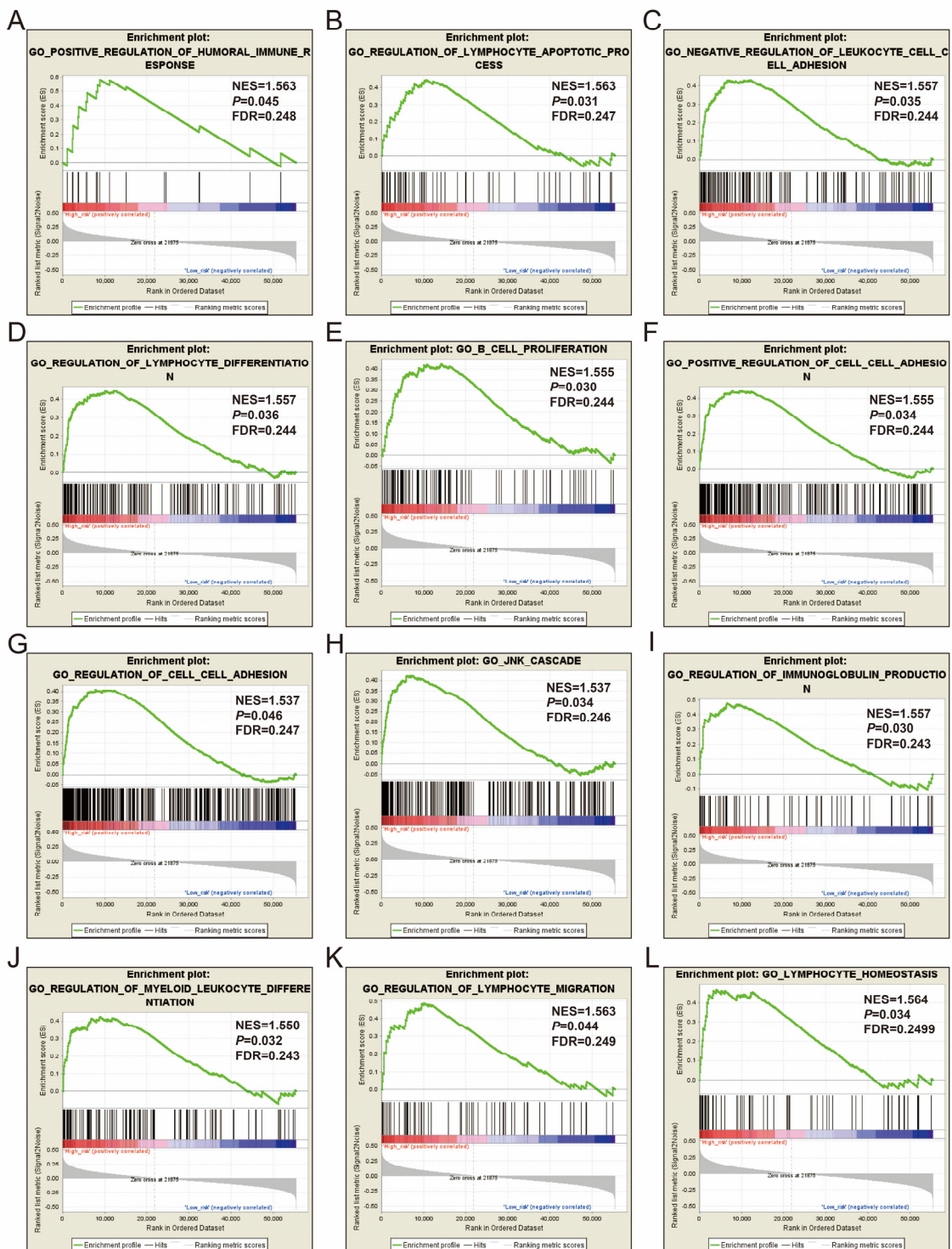


Figure 10. GSEA analysis results of the low- and high-risk score phenotypes in AML using c5 reference gene set. (A) positive regulation of humoral immune response; (B) regulation of lymphocyte apoptotic process; (C) negative regulation of leukocyte cell-cell adhesion; (D) regulation of lymphocyte differentiation; (E) B cell proliferation; (F) positive regulation of cell-cell adhesion; (G) regulation of cell-cell adhesion; (H) JNK cascade; (I) regulation of immunoglobulin production; (J) regulation of myeloid leukocyte differentiation; (K) regulation of lymphocyte migration; (L) lymphocyte homeostasis.

In order to further understand the differential biological functions and pathways between high- and low-risk phenotypes, we also screened for differentially expressed genes between the two phenotypes and performed functional enrichment. By screening, we obtained a total of 185 DEGs between high- and low-risk phenotypes (Figure 11, Table S7 and Figure S1). Through functional enrichment, we found that these DEGs can be significantly enriched in cellular response to retinoic acid, positive regulation of cell proliferation, gamma-aminobutyric acid type A receptor subunit alpha1 (GABA-A) receptor complex, cell junction, cell surface receptor signaling pathway, ephrin receptor signaling pathway, gamma-aminobutyric acid signaling pathway, extracellular matrix (ECM)-receptor interaction, phosphatidylinositol 3-kinase (PI3K)-Akt signaling pathway and proteoglycans in cancer (Figure 12, Table S8). We also use these DEGs to conduct potential AML targeted drug screening in CMap. We have screened a total of six small molecule drugs that may be potential targeted therapies for AML. These six drugs are alimemazine, MG-262, fluoxetine, quipazine, naltrexone and oxybenzone (Figure 13A–G). In the analysis of the Drug-gene interaction network constructed by STITCH, we found that fluoxetine can play a targeted therapeutic role in AML by participating in the regulation of solute carrier family 6 member 2 (SLC6A2) and cytochrome P450 family 2 subfamily C member 9 (CYP2C9) (Figure 14). In addition, Quipazine is also involved in the regulation of SLC6A2 in AML (Figure 14). In addition, we also found that naltrexone plays a targeted therapeutic role in AML through gamma-aminobutyric acid type A receptor subunit alpha2 (GABRA2) and oxybenzone through potassium voltage-gated channel interacting protein 1 (KCNIP1) (Figure 14). Finally, we used multivariate Cox proportional hazard regression model to analyze the prognostic values of these DEGs in R platform, and we screened a total of 28 DEGs that were significantly related to the prognosis of AML (Figure 15A, Table S9). The top three genes with the most significant P values are matrix metalloproteinase 7 (MMP7) (Figure 15B), SIX homeobox 4 (SIX4) (Figure 15C) and gamma-aminobutyric acid type A receptor subunit epsilon (GABRE) (Figure 15D).

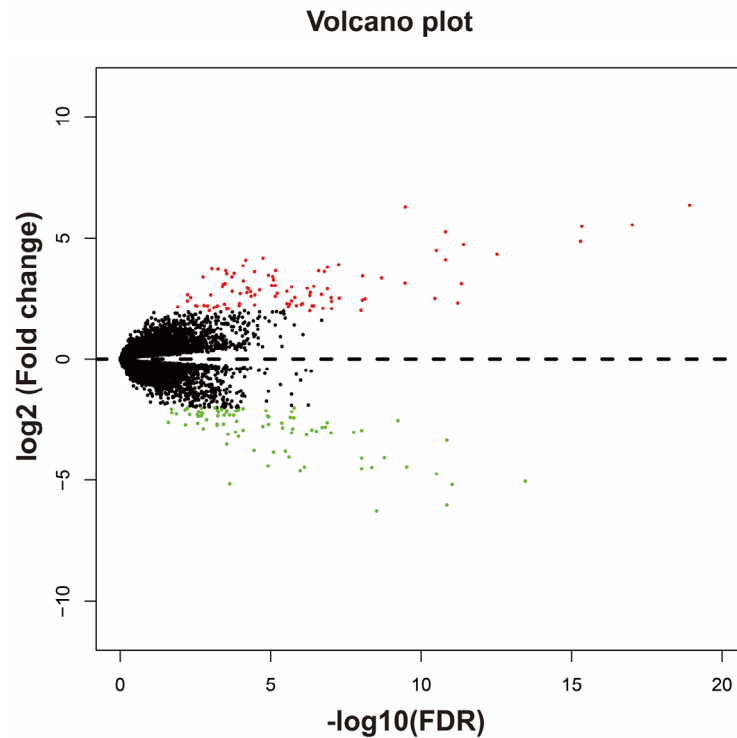


Figure 11. Volcano plot of the differentially expressed genes between the low- and high-risk score phenotypes of AML.

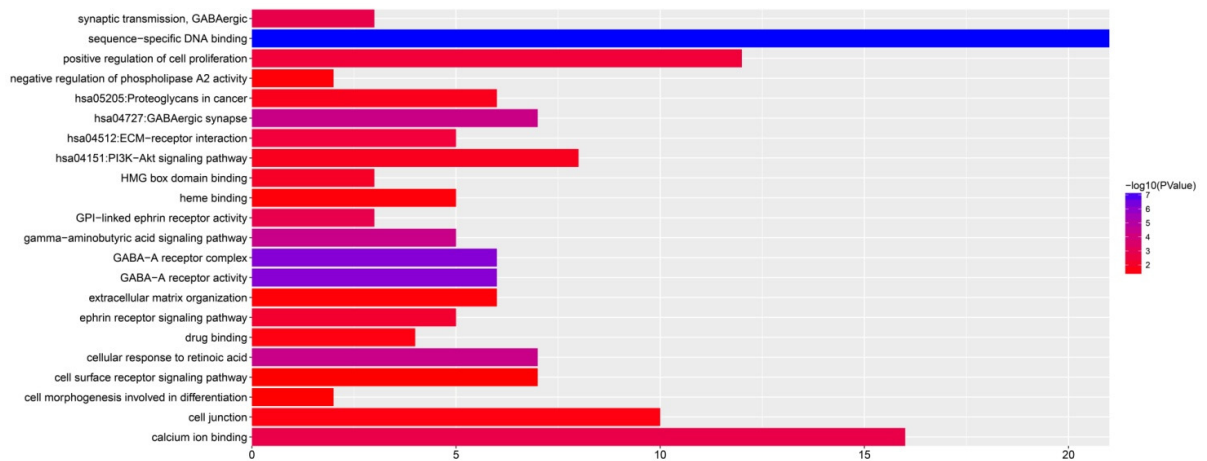


Figure 12. Functional enrichment results of the differentially expressed genes between the low- and high-risk score phenotypes of AML.

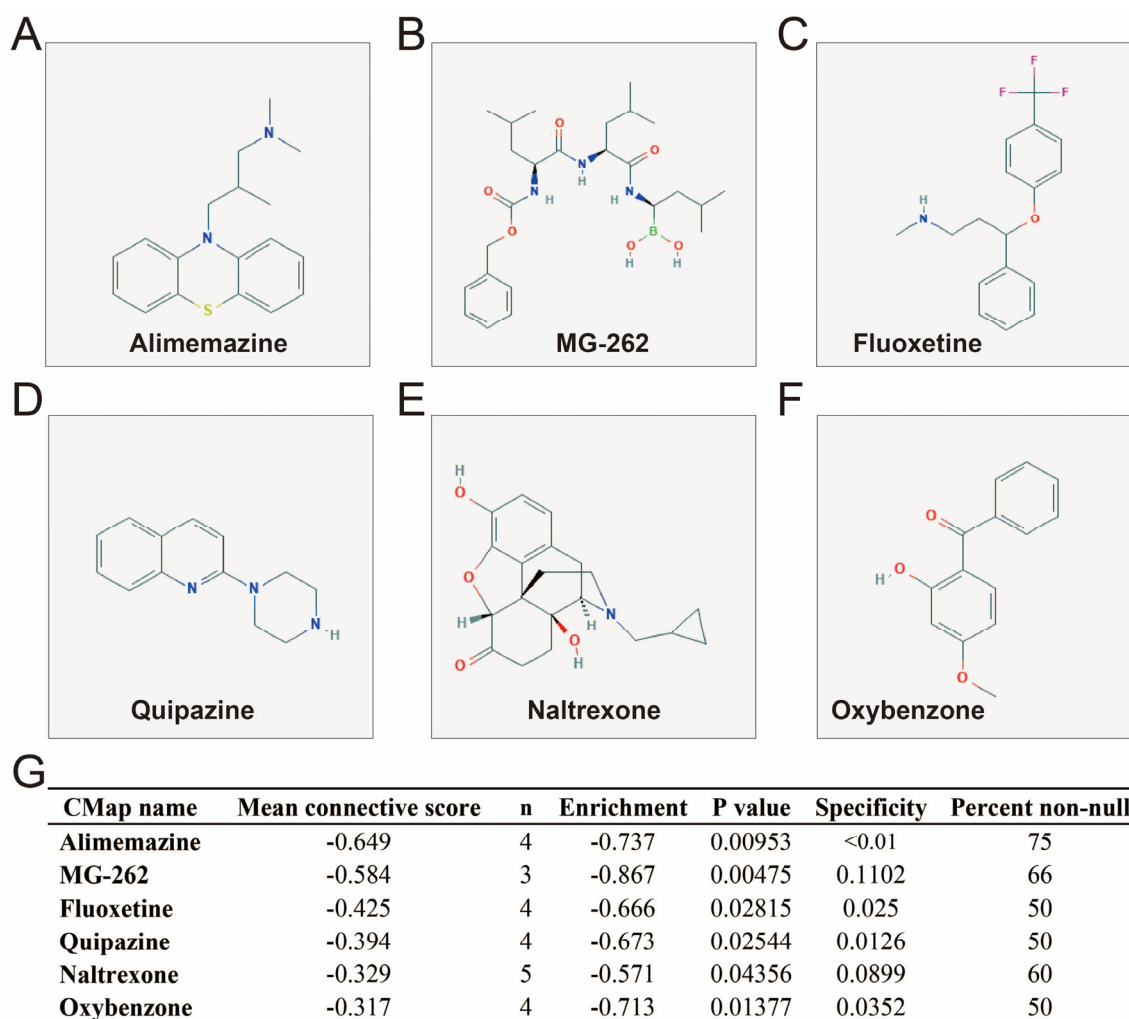


Figure 13. CMap analysis results of the low- and high-risk score phenotypes in AML. (A) The chemical structure of alimemazine; (B) The chemical structure of MG-262; (C) The chemical structure of fluoxetine; (D) The chemical structure of quipazine; (E) The chemical structure of naltrexone; (F) The chemical structure of oxybenzone; (G) The list of CMap analysis results.

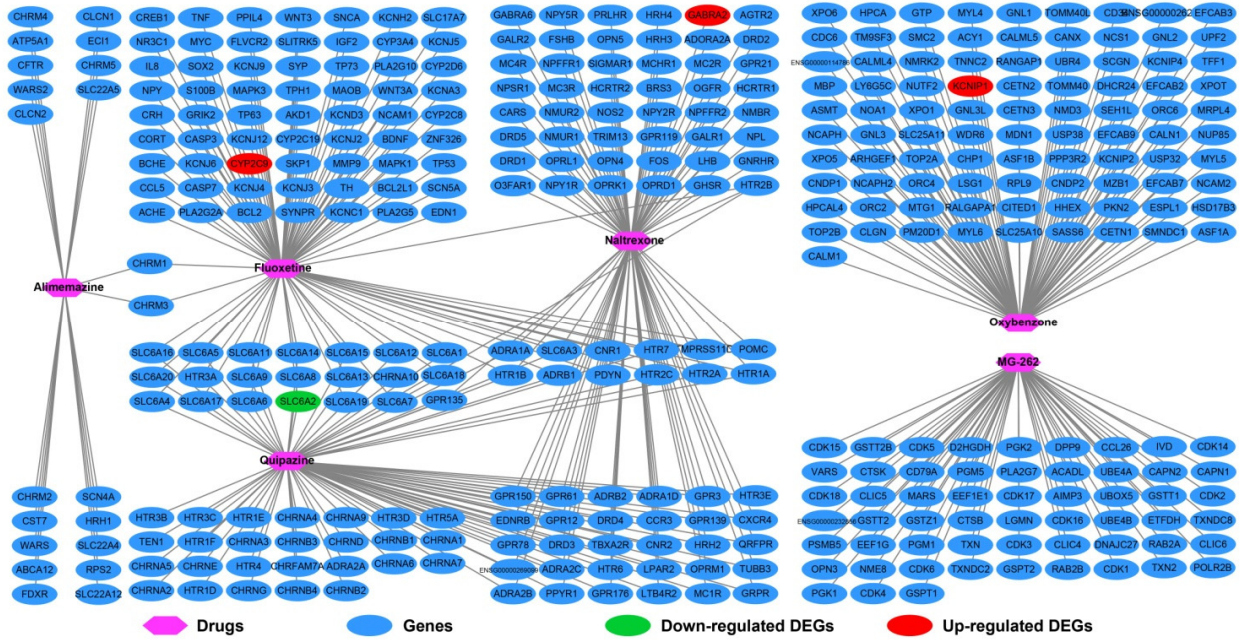


Figure 14. Drug-gene interaction networks of six drugs.

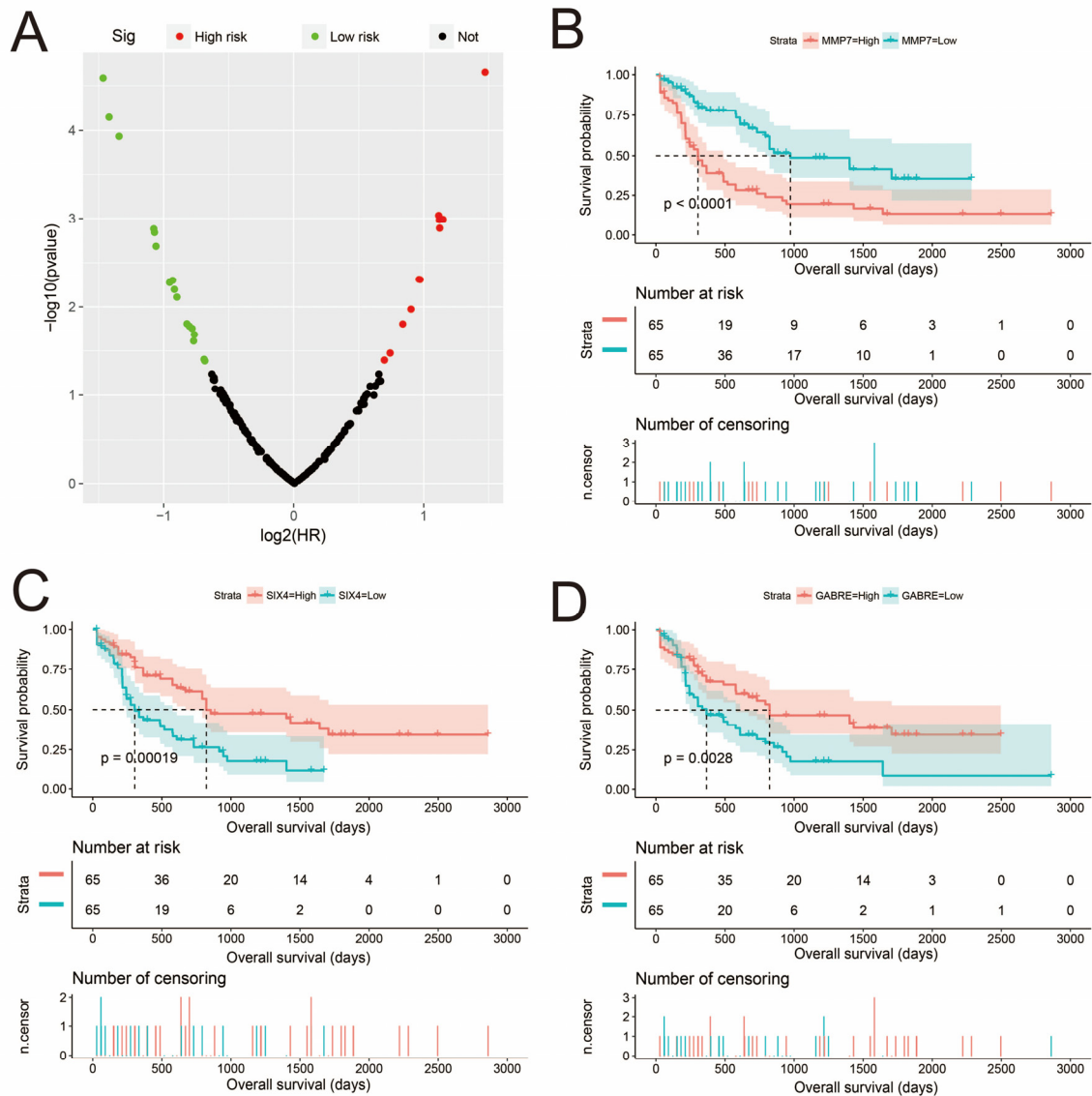


Figure 15. Survival analysis results of the differentially expressed genes between the low- and high-risk score phenotypes of AML. (A) Volcano plot of the survival results; (B) Kaplan-Meier curve of MMP7; (C) Kaplan-Meier curve of SIX4; (D) Kaplan-Meier curve of GABRE.

3.4. Immune microenvironment and infiltration analysis

By calculating the scores of stromal cells and immune cells in the immune microenvironment, we found that there are significant differences in AML patients at different risks in their immune and ESTIMATE scores, and AML patients with high risk score have higher immune scores and ESTIMATE scores (Figure 16A–C). No significant difference was observed in the stromal score between the two risk score of AML patients (Figure 16A). By plotting a histogram of immune cell infiltration in AML patients, we can clearly understand the proportion of immune cells in AML patients (Figure 17A). Furthermore, we observed that there is significant differences in mast cell resting infiltration between AML patients with different risk score (Figure 17B).

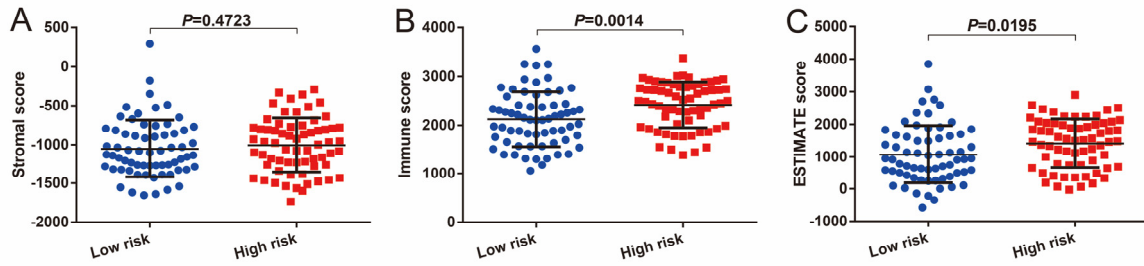


Figure 16. Scatter plot of immune microenvironment score in TCGA AML cohort. (A) Stromal score; (B) Immune score; (C) ESTIMATE score.

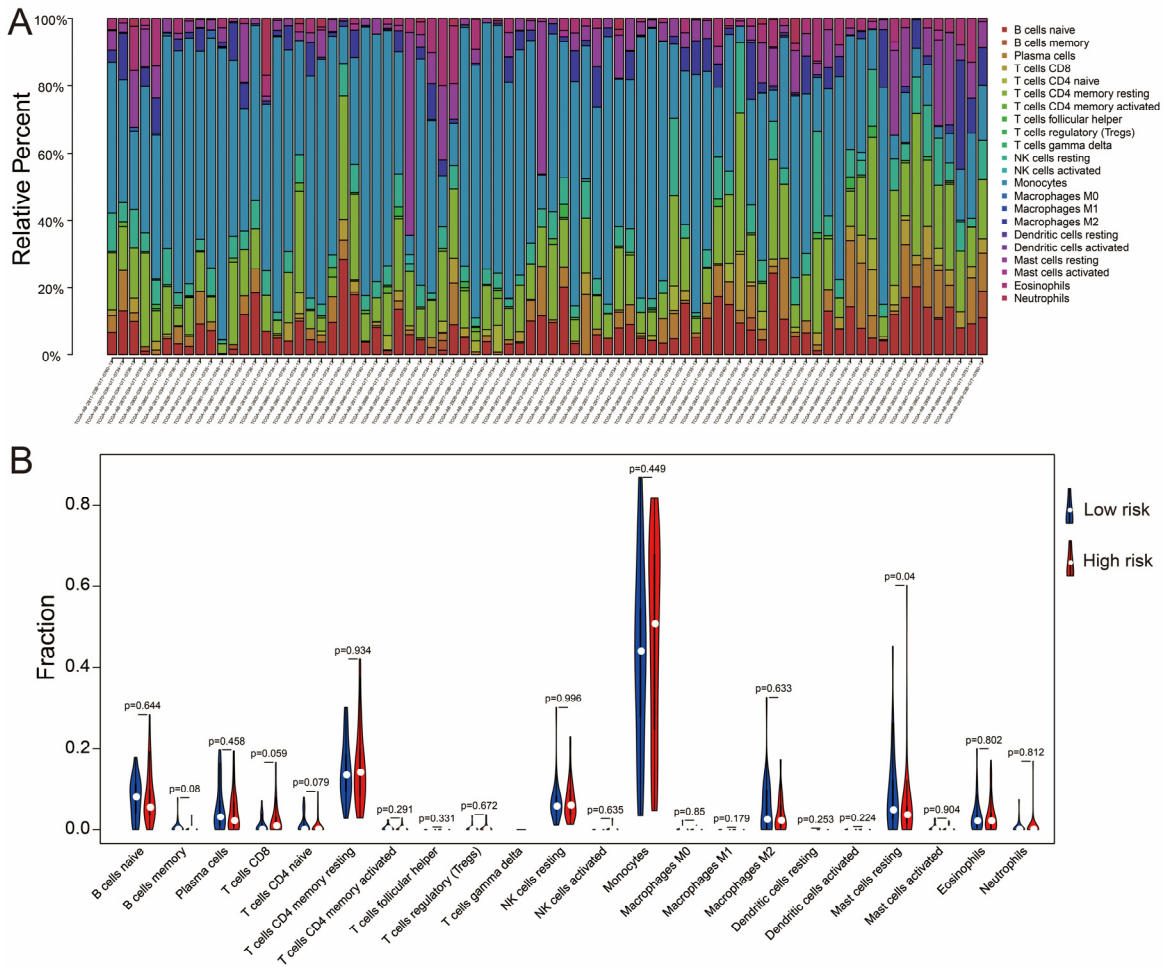


Figure 17. Demonstration of analysis of immune cell infiltration results in TCGA AML cohort. (A) Histogram of the proportion of immune cells; (B) Violin plot of immune cells between AML patients with different risk scores.

4. Discussion

With the discovery of high-throughput sequencing technology, more and more studies have shown that snoRNAs is closely related to the prognosis of cancers. Huang et al. identified several

snoRNAs significantly related to the prognosis of colon adenocarcinoma by analyzing the TCGA RNA-seq dataset, and constructed a prognosis signature consisting of two snoRNAs expressions [14]. Similar to the research by Huang et al., Xing et al. identified snoRNAs of 113 snoRNAs significantly related to the prognosis of HNSC by using the RNA-seq dataset of the TCGA head and neck squamous cell carcinoma (HNSC) cohort, and used the least absolute shrinkage and selection operator (LASSO) regression to construct a prognostic signature that included 5 prognostic snoRNAs, which can significantly divide HNSC patients into high- and low-risk phenotypes [12]. In addition, Zhao et al. used TCGA ccRCC RNA-seq dataset to identify a 6snoRNA signature for ccRCC diagnosis and prognosis prediction [13]. Based on the above research, this study used the TCGA sequencing dataset to screen snoRNAs related to AML prognosis. We identified a total of 30 snoRNAs that were significantly related to the prognosis of AML, and constructed an AML prognostic signature containing 14 prognostic snoRNAs based on the above results, which can accurately predict the 5-year survival of AML patients.

For the above 14 prognostic snoRNAs, some of them have also been reported to be closely related to cancers in previous studies. Ronchetti et al. screened the expression profile of sno/scaRNAs in patients with chronic lymphocytic leukemia (CLL) and found that SNORA31 is down-regulated in CLL, which may be a new biomarker related to CLL [38]. Bignotti et al. found that SNORD72 was significantly upregulated in high-grade serous carcinoma tissues compared with normal control tissues [39]. Mao et al. found that SNORD72 is significantly overexpressed in hepatocellular carcinoma (HCC) tumor tissues, and it plays an oncogene role in HCC. High expression of SNORD72 can significantly promote HCC cell proliferation, colony formation and invasion [40]. Human SNORA31 variations can affect the innate immunity of the central nervous system to herpes simplex virus-1, thereby affecting the occurrence of herpes simplex encephalitis [41]. Davanian et al found that SNORA65 was significantly up-regulated in Ameloblastoma tissue, and the expression level was positively correlated with the tumor size [42].

For the function of the above 14 snoRNAs prognostic signature in AML, we found that this prognostic signature is closely related to some classic tumor-related signaling pathways, including PI3K-Akt, Wnt, EMT, TCR, NF- κ B, mTOR signaling pathways. The PI3K-Akt-mTOR pathway is one of the abnormally up-regulated signaling pathways in cancers, including AML. The increased activity in the PI3K-Akt-mTOR pathway is a poor prognostic indicator of AML. Pharmacological targeting of the PI3K-Akt-mTOR pathway with specific inhibitors can inhibit the growth of AML cells [43–45]. In addition, targeted inhibition of PI3K, mTOR, Erk and Bcl-2 signaling network can also increase the apoptosis of AML, which may be a potential AML targeted therapy strategy [46]. Targeted inhibition of mTOR kinase can be used as a potential strategy for the treatment of AML, and may also affect the resistance of AML to chemotherapy drugs [47]. Targeted inhibition of mTOR in AML cells can significantly reduce cell metabolic activity, block the cell cycle, and induce apoptosis, which may be a potential therapeutic strategy for AML [48–51]. In the process of tumor cell development and development, EMT will also cause tumor cells to lose some of the characteristics of epithelial cells to obtain some of the characteristics of interstitial cells, and also allow tumor cells to acquire stronger invasion and detachment capabilities. Targeted inhibition of EMT in AML cells can significantly reduce the invasiveness of AML, and EMT-related genes are significantly associated with poor prognosis of AML [52]. Zhang et al. found that EMT-related gene E-cadherin is lowly expressed in AML, and ROC analysis suggests that it can be used as a diagnostic biomarker for AML. At the same time, low expression of E-cadherin is also significantly associated with the poor prognosis of AML [53]. High expression of EMT-related gene vimentin is significantly associated with poor prognosis of AML [54]. Zhong et al showed that TCR gene rearrangement can

be used to monitor minimal residual disease in AML patients [55]. Previous studies showed that WT1-specific T cell receptor can be used for the treatment of AML, and can prevent the recurrence of AML after hematopoietic cell transplantation [56,57]. Previous studies have shown that Wnt signaling pathway is necessary to maintain the stem cell characteristics of AML [58,59], and dysregulation of Wnt signaling can alter the microenvironment of AML [60]. Wnt signaling pathway related genes are significantly associated with AML prognosis, and Wnt signaling pathway can be used as a target for AML therapy [59]. Inhibition of the Wnt signaling pathway by the use of Wnt antagonists in AML induces abnormal methylation in AML cells, which is closely associated with recurrence and death of AML patients [61,62]. NF- κ B signaling pathway is closely related to cancer cell apoptosis, tumor genesis, angiogenesis, growth, tumor immunity and metastasis. Monotherapy or combination therapy with NF- κ B inhibitors aimed at preventing NF- κ B activity and inducing apoptosis can be used as a strategy for AML treatment [63–66]. Choi et al.'s research indicates that the instability of the NF- κ B and p38/MAPK signaling pathway is a key factor in the resistance of AML cells to radiotherapy and doxorubicin [67]. Co-suppression of NF- κ B and c-Jun N-terminal kinase can significantly increase the sensitivity of drug therapy in tumor necrosis factor-expressing AML cells [68]. The research of Bosman et al. showed that transforming growth factor- β activated kinase 1 (TAK1) is significantly upregulated in AML, and its inhibitor can induce AML cell apoptosis by blocking NF κ B [69]. Therefore, TAK1-NF- κ B axis can be used as therapeutic target for AML [69].

For the six small molecule drugs screened in this study, we found that some drugs have been reported to be closely related to tumors in previous studies. Ma et al.'s research suggests that low-dose naltrexone can participate in the regulation of Bax/Bcl-2/caspase-3/PARP signaling axis through M1 macrophages, thereby exerting a tumor suppressive effect in colorectal cancer cells [70]. Liu et al.'s study also reported that low-dose naltrexone can exert anti-cancer effects by inhibiting EMT of Hela cells [71]. 1-Naphthyl, a derivative of quipazine, can exert a tumor suppressive effect by inducing oxidative stress in melanoma cells [72]. MG-262, a proteasome inhibitor, which was reported by Wei et al. through CMap analysis and found that MG-262 may be a targeted therapeutic drug for head and neck squamous cell carcinoma [73]. Transcription replication will become an effective target of the proteasome inhibitor MG-262 in cancer chemotherapy, which can enhance the sensitivity of cancer cells to cisplatin, but has little effect on normal cells [74]. Proteasome inhibitors are a new class of anticancer drugs that have recently been introduced into the clinical treatment of multiple myeloma [75]. Zavrski et al. found that proteasome inhibitors, including MG-262, can significantly inhibit the growth of myeloma cells, block the cell cycle and induce apoptosis by using several proteasome inhibitors to intervene in human myeloma cell lines, respectively [76]. Wang et al.'s research suggests that MG-262 can induce ovarian cancer cell apoptosis, inhibit ovarian cancer cell proliferation and angiogenesis through the Erk signaling pathway [77]. Fluoxetine has been reported to have anti-tumor effects. Wu et al. found that fluoxetine can induce non-small cell lung cancer (NSCLC) cell apoptosis and inhibit DNA repair and metastatic potential by activating the NF- κ B signaling pathway [78]. Hsu et al. confirmed via *in vivo* experiments that fluoxetine in hepatocellular carcinoma (HCC) and NSCLC can significantly reduce tumor cell proliferation, induce apoptosis, and regulate the expression of invasion-related proteins. Its potential mechanism of action in two tumors may be by blocking the activation of Akt/NF- κ B or Erk/NF- κ B signaling pathways [79]. MUN et al. also supported the conclusion that Fluoxetine plays an anti-tumor role in HCC [80]. Sun et al.'s findings suggest that fluoxetine can induce apoptosis and autophagic cell death of Triple negative breast cancer (TNBC) cells by inhibiting eEF2K and activating the AMPK-mTOR-ULK complex axis, which can be used as a potential TNBC treatment strategy [81]. Kabel et al.'s study also supports the conclusion that fluoxetine has an anti-cancer effect in breast

cancer [82]. Fluoxetine also can exert tumor suppressive effect by inducing cytotoxic endoplasmic reticulum stress and autophagy in TNBC [83]. Khing et al found that fluoxetine can significantly enhance the antiproliferative effect of paclitaxel in gastric adenocarcinoma cells, and the combined effect of the two drugs can significantly induce apoptosis and necroptosis [84]. The study of Khin et al. also suggested that fluoxetine has an anti-tumor effect in gastric cancer (GC), which induces apoptosis of GC cells through endoplasmic reticulum stress pathway [85]. Fluoxetine has also been reported that its antitumor effect in colorectal cancer cells mainly induces apoptosis and DNA breakage of colorectal cancer cells through its cytotoxic effect, and its mechanism of inducing apoptosis is p53-independent [86]. Kannen et al. found that fluoxetine can significantly affect the energy production of colorectal cancer tumor cells, and can also induce cell cycle arrest and inhibit cell proliferation, resulting in tumors under hypoxic conditions. Then, hypoxia can lead to reduced microvessel formation and reduced tumor size in the tumor tissue of the colorectal cancer xenograft model [87]. Several studies have also reported that Fluoxetine has antitumor effects in colorectal cancer [88,89]. Koh et al found that Fluoxetine can reduce the risk of experimental colitis-associated colon cancer in mice by participating in the regulation of NF- κ B signaling pathway [90]. Fluoxetine can significantly inhibit the growth of glioblastoma and exert anticancer effect [91,92]. Although fluoxetine exerts antitumor effects in a variety of solid tumors, however, its role on AML has not been reported. Our study is the first to report that fluoxetine may be used as a potential AML targeted therapy drug based on in silico analysis. Through literature search, we have not found any reports about anti-tumor effects of alimemazine and oxybenzone.

This study has some disadvantages that need to be clarified. First, the AML cohort in this study is derived from the TCGA single center cohort, and the sample size is small. Our results still need to be verified in a multi-center cohorts with large sample size. Secondly, many clinical parameters are unavailable due to dataset from TCGA. Third, because this study is a in silico analysis, we used genome-wide dataset to screen out a large number of potential functional mechanisms and targeted therapeutic drugs related to AML, but our results still lacks *in vivo* and *in vitro* functional experimental verification. Despite the aforementioned disadvantages, the advantage of this study is that we are the first to use genome-wide data set to screen prognostic snoRNAs for AML. This study explores the genome of AML from a new perspective, which can provide a theoretical basis for future research. At the same time, this study also identified six potential targeted drugs for AML. Once these drugs are verified *in vivo* and *in vitro* experiments, they can also help in the future treatment of AML. Most importantly, this study also constructed an AML prognostic signature and nomogram model based on snoRNAs expression, which can provide new biomarkers for AML.

5. Conclusions

In conclusion, our current study was constructed an AML prognostic signature based on 14 snoRNAs, and a nomogram model for predicting AML prognosis was constructed based on this signature. Through GSEA, snoRNAs co-expressed PCGs and DEGs functional enrichment analysis, we screened a large number of potential functional mechanisms of this prognostic signature in AML. In the subsequent targeted drug screening, we also identified six small-molecule drugs that can be used for AML targeted therapy. At the same time, we also used drug-gene interaction analysis tools to identify potential targets for some drugs to function in AML. We have also observed that AML patients with different risk scores have significant differences in the immune microenvironment and immune cell infiltration. Although this study is the first to comprehensively analyze the relationship between snoRNAs and AML prognosis

through whole-genome dataset, however, our results still need to be verified by further *in vivo* and *in vitro* functional experiments in future studies.

Acknowledgments

This work was supported in part by the National Natural Science Foundation of China (No.81160075, 81960038); Natural Science Foundation of Guangxi (No.0728124); Self-raised Scientific Research Fund of the Ministry of Health of Guangxi Province (Z2014035). The authors thank the contributors of The Cancer Genome Atlas (<https://portal.gdc.cancer.gov/>) for their contribution to share the AML dataset on open access. In addition, we also would like to acknowledge the helpful comments on this paper received from our reviewers.

Conflict of interest

The authors declare that they have no competing interests.

References

1. A. Khwaja, M. Bjorkholm, R. E. Gale, R. L. Levine, C. T. Jordan, G. Ehninger, et al., Acute myeloid leukaemia, *Nat. Rev. Dis. Primers*, **2** (2016), 16010. <https://doi.org/10.1038/nrdp.2016.10>
2. E. Estey, H. Dohner, Acute myeloid leukaemia, *Lancet*, **368** (2006), 1894–1907. [https://doi.org/10.1016/S0140-6736\(06\)69780-8](https://doi.org/10.1016/S0140-6736(06)69780-8)
3. L. Bullinger, K. Dohner, E. Bair, S. Frohling, R. F. Schlenk, R. Tibshirani, et al., Use of gene-expression profiling to identify prognostic subclasses in adult acute myeloid leukemia, *N. Eng. J. Med.*, **350** (2004), 1605–1616. <https://doi.org/10.1056/NEJMoa031046>
4. E. Papaemmanuil, M. Gerstung, L. Bullinger, V. I. Gaidzik, P. Paschka, N. D. Roberts, et al., Genomic classification and prognosis in acute myeloid leukemia, *N. Eng. J. Med.*, **374** (2016), 2209–2221. <https://doi.org/10.1056/NEJMoa1516192>
5. C. C. Coombs, M. S. Tallman, R. L. Levine, Molecular therapy for acute myeloid leukaemia, *Nat. Rev. Clin. Oncol.*, **13** (2016), 305–318. <https://doi.org/10.1038/nrclinonc.2015.210>
6. J. W. Tyner, C. E. Tognon, D. Bottomly, B. Wilmot, S. E. Kurtz, S. L. Savage, et al., Functional genomic landscape of acute myeloid leukaemia, *Nature*, **562** (2018), 526–531. <https://doi.org/10.1038/s41586-018-0623-z>
7. S. Abelson, G. Collord, S. W. K. Ng, O. Weissbrod, N. M. Cohen, E. Niemeyer, et al., Prediction of acute myeloid leukaemia risk in healthy individuals, *Nature*, **559** (2018), 400–404. <https://doi.org/10.1038/s41586-018-0317-6>
8. S. C. Meyer, R. L. Levine, Translational implications of somatic genomics in acute myeloid leukaemia, *Lancet Oncol.*, **15** (2014), e382–394. [https://doi.org/10.1016/S1470-2045\(14\)70008-7](https://doi.org/10.1016/S1470-2045(14)70008-7)
9. T. Bratkovic, J. Bozic, B. Rogelj, Functional diversity of small nucleolar RNAs, *Nucleic Acids Res.*, **48** (2020), 1627–1651. <https://doi.org/10.1093/nar/gkz1140>
10. J. Ni, A. L. Tien, M. J. Fournier, Small nucleolar RNAs direct site-specific synthesis of pseudouridine in ribosomal RNA, *Cell*, **89** (1997), 565–573. [https://doi.org/10.1016/S0092-8674\(00\)80238-x](https://doi.org/10.1016/S0092-8674(00)80238-x)

11. V. Chikne, K. S. Rajan, M. Shalev-Benami, K. Decker, S. Cohen-Chalamish, H. Madmoni, et al., Small nucleolar RNAs controlling rRNA processing in *Trypanosoma brucei*, *Nucleic Acids Res.*, **47** (2019), 2609–2629. <https://doi.org/10.1093/nar/gky1287>
12. L. Xing, X. Zhang, X. Zhang, D. Tong, Expression scoring of a small-nucleolar-RNA signature identified by machine learning serves as a prognostic predictor for head and neck cancer, *J. Cell Phys.*, **235** (2020), 8071–8084. <https://doi.org/10.1002/jcp.29462>
13. Y. Zhao, Y. Yan, R. Ma, X. Lv, L. Zhang, J. Wang, et al., Expression signature of six-snoRNA serves as novel non-invasive biomarker for diagnosis and prognosis prediction of renal clear cell carcinoma, *J. Cell Mol. Med.*, **24** (2020), 2215–2228. <https://doi.org/10.1111/jcmm.14886>
14. L. Huang, X. Z. Liang, Y. Deng, Y. B. Liang, X. Zhu, X. Y. Liang, et al., Prognostic value of small nucleolar RNAs (snoRNAs) for colon adenocarcinoma based on RNA sequencing data, *Pathol. Res. Pract.*, **216** (2020), 152937. <https://doi.org/10.1016/j.prp.2020.152937>
15. J. Gong, Y. Li, C. J. Liu, Y. Xiang, C. Li, Y. Ye, et al., A pan-cancer analysis of the expression and clinical relevance of small nucleolar RNAs in human cancer, *Cell Rep.*, **21** (2017), 1968–1981. <https://doi.org/10.1016/j.celrep.2017.10.070>
16. The Cancer Genome Atlas Research Network, Genomic and epigenomic landscapes of adult de novo acute myeloid leukemia, *N. Eng. J. Med.*, **368** (2013), 2059–2074. <https://doi.org/10.1056/NEJMoa1301689>
17. M. D. Robinson, D. J. McCarthy, G. K. Smyth, edgeR: a Bioconductor package for differential expression analysis of digital gene expression data, *Bioinformatics*, **26** (2010), 139–140. <https://doi.org/10.1093/bioinformatics/btp616>
18. R. Huang, X. Liao, Q. Li, Identification and validation of potential prognostic gene biomarkers for predicting survival in patients with acute myeloid leukemia, *Oncol. Targets Ther.*, **10** (2017), 5243–5254. <https://doi.org/10.2147/OTT.S147717>
19. X. Liao, X. Wang, K. Huang, C. Yang, T. Yu, C. Han, et al., Genome-scale analysis to identify prognostic microRNA biomarkers in patients with early stage pancreatic ductal adenocarcinoma after pancreaticoduodenectomy, *Cancer Manage. Res.*, **10** (2018), 2537–2551. <https://doi.org/10.2147/CMAR.S168351>
20. X. Liao, X. Wang, K. Huang, C. Han, J. Deng, T. Yu, et al., Integrated analysis of competing endogenous RNA network revealing potential prognostic biomarkers of hepatocellular carcinoma, *J. Cancer*, **10** (2019), 3267–3283. <https://doi.org/10.7150/jca.29986>
21. W. H. Da, B. T. Sherman, R. A. Lempicki, Systematic and integrative analysis of large gene lists using DAVID bioinformatics resources, *Nat. Protoc.*, **4** (2009), 44–57. <https://doi.org/10.1038/nprot.2008.211>
22. V. K. Mootha, C. M. Lindgren, K. F. Eriksson, A. Subramanian, S. Sihag, J. Lehar, et al., PGC-1alpha-responsive genes involved in oxidative phosphorylation are coordinately downregulated in human diabetes, *Nat. Genet.*, **34** (2003), 267–273. <https://doi.org/10.1038/ng1180>
23. A. Subramanian, P. Tamayo, V. K. Mootha, S. Mukherjee, B. L. Ebert, M. A. Gillette, et al., Gene set enrichment analysis: a knowledge-based approach for interpreting genome-wide expression profiles, *Proc. Nat. Acad. Sci. U. S. A.*, **102** (2005), 15545–15550. <https://doi.org/10.1073/pnas.0506580102>

24. A. Liberzon, C. Birger, H. Thorvaldsdottir, M. Ghandi, J. P. Mesirov, P. Tamayo, The molecular signatures database (MSigDB) hallmark gene set collection, *Cell Syst.*, **1** (2015), 417–425. <https://doi.org/10.1016/j.cels.2015.12.004>
25. A. Liberzon, A. Subramanian, R. Pinchback, H. Thorvaldsdottir, P. Tamayo, J. P. Mesirov, Molecular signatures database (MSigDB) 3.0, *Bioinformatics*, **27** (2011), 1739–1740. <https://doi.org/10.1093/bioinformatics/btr260>
26. J. Lamb, The connectivity map: a new tool for biomedical research, *Nat. Rev. Cancer*, **7** (2007), 54–60. <https://doi.org/10.1038/nrc2044>
27. J. Lamb, E. D. Crawford, D. Peck, J. W. Modell, I. C. Blat, M. J. Wrobel, et al., The connectivity map: using gene-expression signatures to connect small molecules, genes, and disease, *Science*, **313** (2006), 1929–1935. <https://doi.org/10.1126/science.1132939>
28. E. W. Sayers, J. Beck, J. R. Brister, E. E. Bolton, K. Canese, D. C. Comeau, et al., Database resources of the national center for biotechnology information, *Nucleic Acids Res.*, **48** (2020), D9–D16. <https://doi.org/10.1093/nar/gkz899>
29. S. Kim, J. Chen, T. Cheng, A. Gindulyte, J. He, S. He, et al., PubChem 2019 update: improved access to chemical data, *Nucleic Acids Res.*, **47** (2019), D1102–D1109. <https://doi.org/10.1093/nar/gky1033>
30. M. Kuhn, D. Szklarczyk, A. Franceschini, M. Campillos, C. V. Mering, L. J. Jensen, et al., STITCH 2: an interaction network database for small molecules and proteins, *Nucleic Acids Res.*, **38** (2010), D552–556. <https://doi.org/10.1093/nar/gkp937>
31. M. Kuhn, C. V. Mering, M. Campillos, L. J. Jensen, P. Bork, STITCH: interaction networks of chemicals and proteins, *Nucleic Acids Res.*, **36** (2008), D684–688. <https://doi.org/10.1093/nar/gkm795>
32. D. Szklarczyk, A. Santos, C. V. Mering, L. J. Jensen, P. Bork, M. Kuhn, STITCH 5: augmenting protein-chemical interaction networks with tissue and affinity data, *Nucleic Acids Res.*, **44** (2016), D380–384. <https://doi.org/10.1093/nar/gkv1277>
33. K. Yoshihara, M. Shahmoradgoli, E. Martinez, R. Vegesna, H. Kim, W. Torres-Garcia, et al., Inferring tumour purity and stromal and immune cell admixture from expression data, *Nat. Commun.*, **4** (2013), 2612. <https://doi.org/10.1038/ncomms3612>
34. B. Chen, M. S. Khodadoust, C. L. Liu, A. M. Newman, A. A. Alizadeh, Profiling tumor infiltrating immune cells with CIBERSORT, *Methods Mol. Biol.*, **1711** (2018), 243–259. https://doi.org/10.1007/978-1-4939-7493-1_12
35. Y. Benjamini, D. Drai, G. Elmer, N. Kafkafi, I. Golani, Controlling the false discovery rate in behavior genetics research, *Behav. Brain Res.*, **125** (2001), 279–284. [https://doi.org/10.1016/s0166-4328\(01\)00297-2](https://doi.org/10.1016/s0166-4328(01)00297-2)
36. P. Shannon, A. Markiel, O. Ozier, N. S. Baliga, J. T. Wang, D. Ramage, et al., Cytoscape: a software environment for integrated models of biomolecular interaction networks, *Genome Res.*, **13** (2003), 2498–2504. <https://doi.org/10.1101/gr.1239303>
37. D. Otasek, J. H. Morris, J. Boucas, A. R. Pico, B. Demchak, Cytoscape automation: empowering workflow-based network analysis, *Genome Biol.*, **20** (2019), 185. <https://doi.org/10.1186/s13059-019-1758-4>
38. D. Ronchetti, L. Mosca, G. Cutrona, G. Tuana, M. Gentile, S. Fabris, et al., Small nucleolar RNAs as new biomarkers in chronic lymphocytic leukemia, *BMC Med. Genomics*, **6** (2013), 27. <https://doi.org/10.1186/1755-8794-6-27>

39. E. Bignotti, S. Calza, R. A. Tassi, L. Zanotti, E. Bandiera, E. Sartori, et al., Identification of stably expressed reference small non-coding RNAs for microRNA quantification in high-grade serous ovarian carcinoma tissues, *J. Cell Mol. Med.*, **20** (2016), 2341–2348. <https://doi.org/10.1111/jcmm.12927>
40. L. H. Mao, S. Y. Chen, X. Q. Li, F. Xu, J. Lei, Q. L. Wang, et al., LncRNA-LALR1 upregulates small nucleolar RNA SNORD72 to promote growth and invasion of hepatocellular carcinoma, *Aging (Albany NY)*, **12** (2020), 4527–4546. <https://doi.org/10.18632/aging.102907>
41. F. G. Lafaille, O. Harschnitz, Y. S. Lee, P. Zhang, M. L. Hasek, G. Kerner, et al., Human SNORA31 variations impair cortical neuron-intrinsic immunity to HSV-1 and underlie herpes simplex encephalitis, *Nat. Med.*, **25** (2019), 1873–1884. <https://doi.org/10.1038/s41591-019-0672-3>
42. H. Davanian, A. Balasiddaiah, R. Heymann, M. Sundstrom, P. Redenstrom, M. Silfverberg, et al., Ameloblastoma RNA profiling uncovers a distinct non-coding RNA signature, *Oncotarget*, **8** (2017), 4530–4542. <https://doi.org/10.18632/oncotarget.13889>
43. I. Nepstad, K. J. Hatfield, I. S. Gronningsaeter, H. Reikvam, The PI3K-Akt-mTOR signaling pathway in human acute myeloid leukemia (AML) cells, *Int. J. Mol. Sci.*, **21** (2020), 2907. <https://doi.org/10.3390/ijms21082907>
44. L. Herschbein, J. L. Liesveld, Dueling for dual inhibition: Means to enhance effectiveness of PI3K/Akt/mTOR inhibitors in AML, *Blood Rev.*, **32** (2018), 235–248. <https://doi.org/10.1016/j.blre.2017.11.006>
45. J. Bertacchini, N. Heidari, L. Mediani, S. Capitani, M. Shahjahani, A. Ahmadzadeh, et al., Targeting PI3K/AKT/mTOR network for treatment of leukemia, *Cell Mol. Life Sci.*, **72** (2015), 2337–2347. <https://doi.org/10.1007/s00018-015-1867-5>
46. Y. Su, X. Li, J. Ma, J. Zhao, S. Liu, G. Wang, et al., Targeting PI3K, mTOR, ERK and Bcl-2 signaling network shows superior antileukemic activity against AML ex vivo, *Biochem. Pharmacol.*, **148** (2018), 13–26. <https://doi.org/10.1016/j.bcp.2017.11.022>
47. Y. Tabe, A. Tafuri, K. Sekihara, H. Yang, M. Konopleva, Inhibition of mTOR kinase as a therapeutic target for acute myeloid leukemia, *Expert Opin. Ther. Targets*, **21** (2017), 705–714. <https://doi.org/10.1080/14728222.2017.1333600>
48. N. Guo, M. Azadniv, M. Coppage, M. Nemer, J. Mendler, M. Becker, et al., Effects of neddylation and mTOR inhibition in acute myelogenous leukemia, *Transl. Oncol.*, **12** (2019), 602–613. <https://doi.org/10.1016/j.tranon.2019.01.001>
49. J. Wu, G. Hu, Y. Dong, R. Ma, Z. Yu, S. Jiang, et al., Matrine induces Akt/mTOR signalling inhibition-mediated autophagy and apoptosis in acute myeloid leukaemia cells, *J. Cell Mol. Med.*, **21** (2017), 1171–1181. <https://doi.org/10.1111/jcmm.13049>
50. Y. Feng, L. Wu, mTOR up-regulation of PFKFB3 is essential for acute myeloid leukemia cell survival, *Biochem. Biophys. Res. Commun.*, **483** (2017), 897–903.
51. J. Bertacchini, C. Frasson, F. Chiarini, D. D’Avella, B. Accordi, L. Anselmi, et al., Dual inhibition of PI3K/mTOR signaling in chemoresistant AML primary cells, *Adv. Biol. Regul.*, **68** (2018), 2–9. <https://doi.org/10.1016/j.jbior.2018.03.001>
52. V. Stavropoulou, S. Kaspar, L. Brault, M. A. Sanders, S. Juge, S. Morettini, et al., MLL-AF9 expression in hematopoietic stem cells drives a highly invasive AML expressing EMT-related genes linked to poor outcome, *Cancer Cell*, **30** (2016), 43–58. <https://doi.org/10.1016/j.ccell.2016.05.011>

53. T. J. Zhang, J. D. Zhou, J. C. Ma, Z. Q. Deng, Z. Qian, D. M. Yao, et al., CDH1 (E-cadherin) expression independently affects clinical outcome in acute myeloid leukemia with normal cytogenetics, *Clin. Chem. Lab. Med.*, **55** (2017), 123–131. <https://doi.org/10.1515/cclm-2016-0205>
54. S. Wu, Y. Du, J. Beckford, H. Alachkar, Upregulation of the EMT marker vimentin is associated with poor clinical outcome in acute myeloid leukemia, *J. Transl. Med.*, **16** (2018), 170. <https://doi.org/10.1186/s12967-018-1539-y>
55. L. Zhong, J. Chen, X. Huang, Y. Li, T. Jiang, Monitoring immunoglobulin heavy chain and T-cell receptor gene rearrangement in cfDNA as minimal residual disease detection for patients with acute myeloid leukemia, *Oncol. Lett.*, **16** (2018), 2279–2288. <https://doi.org/10.3892/ol.2018.8966>
56. A. G. Chapuis, D. N. Egan, M. Bar, T. M. Schmitt, M. S. McAfee, K. G. Paulson, et al., T cell receptor gene therapy targeting WT1 prevents acute myeloid leukemia relapse post-transplant, *Nat. Med.*, **25** (2019), 1064–1072. <https://doi.org/10.1038/s41591-019-0472-9>
57. H. J. Stauss, S. Thomas, M. Cesco-Gaspere, D. P. Hart, S. A. Xue, A. Holler, et al., WT1-specific T cell receptor gene therapy: improving TCR function in transduced T cells, *Blood Cells Mol. Dis.*, **40** (2008), 113–116. <https://doi.org/10.1016/j.bcmd.2007.06.018>
58. Y. Wang, A. V. Krivtsov, A. U. Sinha, T. E. North, W. Goessling, Z. Feng, et al., The Wnt/beta-catenin pathway is required for the development of leukemia stem cells in AML, *Science*, **327** (2010), 1650–1653. <https://doi.org/10.1126/science.1186624>
59. A. M. Gruszka, D. Valli, M. Alcalay, Wnt signalling in acute myeloid leukaemia, *Cells*, **8** (2019), 1403. <https://doi.org/10.3390/cells8111403>
60. F. J. Staal, F. Famili, L. G. Perez, K. Pike-Overzet, Aberrant Wnt signaling in leukemia, *Cancers (Basel)*, **8** (2016), 78. <https://doi.org/10.3390/cancers8090078>
61. A. Valencia, J. Roman-Gomez, J. Cervera, E. Such, E. Barragan, P. Bolufer, et al., Wnt signaling pathway is epigenetically regulated by methylation of Wnt antagonists in acute myeloid leukemia, *Leukemia*, **23** (2009), 1658–1666. <https://doi.org/10.1038/leu.2009.86>
62. E. A. Griffiths, S. D. Gore, C. Hooker, M. A. McDevitt, J. E. Karp, B. D. Smith, et al., Acute myeloid leukemia is characterized by Wnt pathway inhibitor promoter hypermethylation, *Leuk. Lymphoma*, **51** (2010), 1711–1719. <https://doi.org/10.3109/10428194.2010.496505>
63. C. Gasparini, C. Celeghini, L. Monasta, G. Zauli, NF-kappaB pathways in hematological malignancies, *Cell Mol. Life Sci.*, **71** (2014), 2083–2102. <https://doi.org/10.1007/s00018-013-1545-4>
64. M. Breccia, G. Alimena, NF-kappaB as a potential therapeutic target in myelodysplastic syndromes and acute myeloid leukemia, *Expert Opin. Ther. Targets*, **14** (2010), 1157–1176. <https://doi.org/10.1517/14728222.2010.522570>
65. M. C. Bosman, J. J. Schuringa, E. Vellenga, Constitutive NF-kappaB activation in AML: Causes and treatment strategies, *Crit. Rev. Oncol. Hematol.*, **98** (2016), 35–44. <https://doi.org/10.1016/j.critrevonc.2015.10.001>
66. J. Zhou, Y. Q. Ching, W. J. Chng, Aberrant nuclear factor-kappa B activity in acute myeloid leukemia: from molecular pathogenesis to therapeutic target, *Oncotarget*, **6** (2015), 5490–5500. <https://doi.org/10.18632/oncotarget.3545>
67. C. H. Choi, H. Xu, H. Bark, T. B. Lee, J. Yun, S. I. Kang, et al., Balance of NF-kappaB and p38 MAPK is a determinant of radiosensitivity of the AML-2 and its doxorubicin-resistant cell lines, *Leuk. Res.*, **31** (2007), 1267–1276. <https://doi.org/10.1016/j.leukres.2006.11.006>

68. A. Volk, J. Li, J. Xin, D. You, J. Zhang, X. Liu, et al., Co-inhibition of NF-kappaB and JNK is synergistic in TNF-expressing human AML, *J. Exp. Med.*, **211** (2014), 1093–1108. <https://doi.org/10.1084/jem.20130990>
69. M. C. Bosman, H. Schepers, J. Jaques, A. Z. Brouwers-Vos, W. J. Quax, J. J. Schuringa, et al., The TAK1-NF-kappaB axis as therapeutic target for AML, *Blood*, **124** (2014), 3130–3140. <https://doi.org/10.1182/blood-2014-04-569780>
70. M. Ma, X. Wang, N. Liu, F. Shan, Y. Feng, Low-dose naltrexone inhibits colorectal cancer progression and promotes apoptosis by increasing M1-type macrophages and activating the Bax/Bcl-2/caspase-3/PARP pathway, *Int. Immunopharmacol.*, **83** (2020), 106388. <https://doi.org/10.1016/j.intimp.2020.106388>
71. N. Liu, M. Ma, N. Qu, R. Wang, H. Chen, F. Hu, et al., Low-dose naltrexone inhibits the epithelial-mesenchymal transition of cervical cancer cells in vitro and effects indirectly on tumor-associated macrophages in vivo, *Int. Immunopharmacol.*, **86** (2020), 106718. <https://doi.org/10.1016/j.intimp.2020.106718>
72. A. C. Menezes, M. Carneiro, J. M. P. F. de Oliveira, A. Ascenso, H. Oliveira, Cytotoxic effect of the serotonergic drug 1-(1-Naphthyl)piperazine against melanoma cells, *Toxicol. Int. Vitro*, **47** (2018), 72–78. <https://doi.org/10.1016/j.tiv.2017.11.011>
73. G. G. Wei, L. Gao, Z. Y. Tang, P. Lin, L. B. Liang, J. J. Zeng, et al., Drug repositioning in head and neck squamous cell carcinoma: An integrated pathway analysis based on connectivity map and differential gene expression, *Pathol. Res. Pract.*, **215** (2019), 152378. <https://doi.org/10.1016/j.prp.2019.03.007>
74. J. Takezawa, Y. Ishimi, K. Yamada, Proteasome inhibitors remarkably prevent translesion replication in cancer cells but not normal cells, *Cancer Sci.*, **99** (2008), 863–871. <https://doi.org/10.1111/j.1349-7006.2008.00764.x>
75. P. G. Richardson, C. Mitsiades, T. Hideshima, K. C. Anderson, Bortezomib: proteasome inhibition as an effective anticancer therapy, *Annu. Rev. Med.*, **57** (2006), 33–47. <https://doi.org/10.1146/annurev.med.57.042905.122625>
76. I. Zavrski, C. Naujokat, K. Niemoller, C. Jakob, U. Heider, C. Langelotz, et al., Proteasome inhibitors induce growth inhibition and apoptosis in myeloma cell lines and in human bone marrow myeloma cells irrespective of chromosome 13 deletion, *J. Cancer Res. Clin. Oncol.*, **129** (2003), 383–391. <https://doi.org/10.1007/s00432-003-0454-6>
77. W. X. Wang, B. H. Kong, P. Li, K. Song, X. Qu, B. X. Cui, et al., Effect of extracellular signal regulated kinase signal pathway on apoptosis induced by MG262 in ovarian cancer cells, *Zhonghua Fu Chan Ke Za Zhi*, **43** (2008), 690–694
78. J. Y. Wu, S. S. Lin, F. T. Hsu, J. G. Chung, Fluoxetine inhibits DNA repair and NF-kB-modulated metastatic potential in non-small cell lung cancer, *Anticancer Res.*, **38** (2018), 5201–5210. <https://doi.org/10.21873/anticancer.12843>
79. L. C. Hsu, H. F. Tu, F. T. Hsu, P. F. Yueh, I. T. Chiang, Beneficial effect of fluoxetine on anti-tumor progression on hepatocellular carcinoma and non-small cell lung cancer bearing animal model, *Biomed. Pharmacother.*, **126** (2020), 110054. <https://doi.org/10.1016/j.biopha.2020.110054>
80. A. R. Mun, S. J. Lee, G. B. Kim, H. S. Kang, J. S. Kim, S. J. Kim, Fluoxetine-induced apoptosis in hepatocellular carcinoma cells, *Anticancer Res.*, **33** (2013), 3691–3697

81. D. Sun, L. Zhu, Y. Zhao, Y. Jiang, L. Chen, Y. Yu, et al., Fluoxetine induces autophagic cell death via eEF2K-AMPK-mTOR-ULK complex axis in triple negative breast cancer, *Cell Prolif.*, **51** (2018), e12402. <https://doi.org/10.1111/cpr.12402>
82. A. M. Kabel, A. A. Elkhoely, Ameliorative potential of fluoxetine/raloxifene combination on experimentally induced breast cancer, *Tissue Cell*, **48** (2016), 89–95. <https://doi.org/10.1016/j.tice.2016.02.002>
83. M. Bowie, P. Pilie, J. Wulfkuhle, S. Lem, A. Hoffman, S. Desai, et al., Fluoxetine induces cytotoxic endoplasmic reticulum stress and autophagy in triple negative breast cancer, *World J. Clin. Oncol.*, **6** (2015), 299–311. <https://doi.org/10.5306/wjco.v6.i6.299>
84. T. M. Khing, W. W. Po, U. D. Sohn, Fluoxetine enhances anti-tumor activity of paclitaxel in gastric adenocarcinoma cells by triggering apoptosis and necroptosis, *Anticancer Res.*, **39** (2019), 6155–6163. <https://doi.org/10.21873/anticancer.13823>
85. P. P. Khin, W. W. Po, W. Thein, U. D. Sohn, Apoptotic effect of fluoxetine through the endoplasmic reticulum stress pathway in the human gastric cancer cell line AGS, *Naunyn Schmiedebergs Arch. Pharmacol.*, **393** (2020), 537–549. <https://doi.org/10.1007/s00210-019-01739-7>
86. M. Marcinkute, S. Afshinjavid, A. A. Fatokun, F. A. Javid, Fluoxetine selectively induces p53-independent apoptosis in human colorectal cancer cells, *Eur. J. Pharmacol.*, **857** (2019), 172441. <https://doi.org/10.1016/j.ejphar.2019.172441>
87. V. Kannen, S. B. Garcia, W. A. Silva, M. Gasser, R. Monch, E. J. Alho, et al., Oncostatic effects of fluoxetine in experimental colon cancer models, *Cell Signal*, **27** (2015), 1781–1788. <https://doi.org/10.1016/j.cellsig.2015.05.008>
88. V. Kannen, H. Hintzsche, D. L. Zanette, W. A. Silva, S. B. Garcia, A. M. Waaga-Gasser, et al., Antiproliferative effects of fluoxetine on colon cancer cells and in a colonic carcinogen mouse model, *PLoS One*, **7** (2012), e50043. <https://doi.org/10.1371/journal.pone.0050043>
89. H. Stopper, S. B. Garcia, A. M. Waaga-Gasser, V. Kannen, Antidepressant fluoxetine and its potential against colon tumors, *World J. Gastrointest. Oncol.*, **6** (2014), 11–21. <https://doi.org/10.4251/wjgo.v6.i1.11>
90. S. J. Koh, J. M. Kim, I. K. Kim, N. Kim, H. C. Jung, I. S. Song, et al., Fluoxetine inhibits NF-kappaB signaling in intestinal epithelial cells and ameliorates experimental colitis and colitis-associated colon cancer in mice, *Am. J. Physiol. Gastrointest. Liver Phys.*, **301** (2011), G9–19. <https://doi.org/10.1152/ajpgi.00267.2010>
91. K. H. Liu, S. T. Yang, Y. K. Lin, J. W. Lin, Y. H. Lee, J. Y. Wang, et al., Fluoxetine, an antidepressant, suppresses glioblastoma by evoking AMPAR-mediated calcium-dependent apoptosis, *Oncotarget*, **6** (2015), 5088–5101. <https://doi.org/10.18632/oncotarget.3243>
92. J. Ma, Y. R. Yang, W. Chen, M. H. Chen, H. Wang, X. D. Wang, et al., Fluoxetine synergizes with temozolomide to induce the CHOP-dependent endoplasmic reticulum stress-related apoptosis pathway in glioma cells, *Oncol. Rep.*, **36** (2016), 676–684. <https://doi.org/10.3892/or.2016.4860>

